






# Paleoecological niche modeling of *Epiophlebia* (Epiophlebioptera: Epiophlebiidae) reveals continuous distribution during the Last Glacial Maximum

Aaron M. Goodman <sup>a,b,c,\*</sup>, Christopher D. Beatty <sup>a,d</sup>, Sebastian Büsse <sup>e</sup>,  
Hidenori Ubukata<sup>f</sup>, Toshiyuki Miyazaki<sup>g</sup>, Mary E. Blair <sup>h</sup> & Jessica L. Ware <sup>a,b</sup>

<sup>a</sup> American Museum of Natural History, Division of Invertebrate Zoology, NY, NY, 10024

<sup>b</sup> Richard Gilder Graduate School, Department of Invertebrate Zoology, American Museum of Natural History, NY, NY, USA, 10024

<sup>c</sup> Graduate School and University Center, City University of New York, NY, NY, 10016

<sup>d</sup> Department of Biology, Stanford University, Stanford, CA, USA

<sup>e</sup> Department of Cytology and Evolutionary Biology, Zoological Institute and Museum, University of Greifswald, Germany

<sup>f</sup> Professor Emeritus, Hokkaido University of Education, Sapporo, Japan

<sup>g</sup> Kansai Research Group of Odonatology, Osaka, Japan

<sup>h</sup> Center for Biodiversity and Conservation, the American Museum of Natural History, New York, NY, USA, 10024

\*Corresponding author: Email: [agoodman@amnh.org](mailto:agoodman@amnh.org)

## Research Article

### OPEN ACCESS

This article is distributed under the terms of the [Creative Commons Attribution License](https://creativecommons.org/licenses/by/4.0/), which permits unrestricted use, distribution, and reproduction in any medium, provided the original author and source are credited.

**Published:** 5 March 2024

**Received:** 8 August 2023

**Accepted:** 22 February 2024

### Citation:

Goodman, Beatty, Büsse, Ubukata, Miyazaki, Blair & Ware (2024): Paleoecological niche modeling of *Epiophlebia* (Epiophlebioptera: Epiophlebiidae) reveals continuous distribution during the Last Glacial Maximum.

*International Journal of Odonatology*, 27, 60–76

doi:10.48156/1388.2024.1917262

### Data Availability Statement:

All relevant data are within the paper and its [Supporting Information files](#).

**Abstract.** Disjunct biogeographic patterns of similar species remain enigmatic within evolutionary biology. Disparate distributions typically reflect species responses to major historical events including past climate change, tectonics, dispersal, and local extinction. Paleo-ecological niche modeling (PaleoENM) has proven useful in inferring the causes of disjunct distributions within charismatic and well-studied taxa including mammals, plants, and birds, but remains under-explored in insects. The relictual Asian dragonfly genus *Epiophlebia* (Suborder Epiophlebioptera: Epiophlebiidae) allows us a novel opportunity to explore PaleoENM in the context of disjunct distributions due to their endemism to the Japanese islands, Himalayas, China, and North Korea. The aim of this paper is to investigate the potential causes behind the modern distribution of *Epiophlebia* by inferring the historical range of these species within the Last Glacial Maximum (LGM), thereby highlighting the utility of PaleoENM in the context of odonate biogeography. Our results indicate possible past routes of gene flow of *Epiophlebia* during the LGM due to high habitat suitability of the genus stretching from the Himalayas to Japan. Furthermore, our results predict several unsampled areas which have the potential to harbor new populations of the genus.

**Key words.** Odonata, Anisozygoptera, dragonfly, Eiprocta, *Epiophlebia*, Ecological Niche Modeling, Maxent

## Introduction

Dragonflies and damselflies (Order: Odonata Fabricius, 1793) represent an overlooked yet invaluable study system for systematics, ecology, and biogeography (Córdoba-Aguilar et al., 2023). Their evolutionary history stretches back ~ 360 mya, with ~ 6405 extant and fossil species currently described (<https://www.odonata-central.org/app/#/wol/>, accessed July 25<sup>th</sup> 2023; Nicholson et al., 2014). Habitats range from single-stream endemics to transoceanic pandemics, and odonate natural history connects both freshwater and terrestrial habitats (Collen et al.,

2014). Furthermore, odonates are considered among the earliest flying insects, a pivotal moment in insect evolution (Dudley & Yanoviak, 2011). Finally, Odonata possess some of the most complex visual color systems, visual acuity, and flight patterns on Earth (Futahashi et al., 2015).

Odonata are divided into three suborders, dragonflies (Anisoptera Sélys, 1854), damselflies (Zygoptera Sélys, 1854), and the enigmatic taxon *Epiophlebia*, Calvert, 1903. *Epiophlebia* are considered relict species due to the unique assortment of characters they share with both Zygoptera and Anisoptera (Asahina, 1954; Büsse, 2016; Davies, 1992; Mahato, 1993), and are hypothesized to represent the most ancestral character states of extant Odonata (Blanke et al., 2013, 2015; Büsse, 2016; Büsse et al., 2015). However, the taxonomic placement of *Epiophlebia* in relation to the other two odonate suborders has remained contentious over the past 110 years (Asahina, 1954; Büsse & Ware, 2022; S. Bybee et al., 2016; S. M. Bybee et al., 2008, 2021; Dijkstra et al., 2013; Nel, 1993). Previously, *Epiophlebia* along with several Jurassic fossils formed the group Anisozygoptera (Nel, 1993), until it was shown that the suborder was polyphyletic (Lohmann, 1996; Rehn, 2003). Currently, *Epiophlebia* is hypothesized to be sister to Anisoptera, along with several extinct lineages forming the monophyletic group Epiprocta (Bechly, 1996a, 1996b; Fleck et al., 2013; Grimaldi et al., 2005; Rehn, 2003). Numerous phylogenetic studies utilizing both molecular and morphological characters support the validity of Epiprocta (Blanke et al., 2013, 2015; Kohli et al., 2021; Letsch et al., 2016).

Currently, *Epiophlebia* contains three species: *Epiophlebia superstes* (Sélys-Longchamps, 1889), *Epiophlebia laidlawi* (Tillyard, 1921), and the more recently described *Epiophlebia sinensis* (J. K. Li et al., 2012), all of which are easily identified by a black and yellow striped pattern in coloration (Asahina, 1954). A putative fourth species, *Epiophlebia diana* (Carle, 2012), was demoted to a junior synonym of *Epiophlebia laidlawi* through morphological and phylogenetic analysis (Büsse & Ware, 2022).

Ancestors of *Epiophlebia* were at their highest diversity within the Mesozoic across the pre-Asian continent (Nel, 1993), with extant *Epiophlebia* being considered as relictual due to their disparate distribution and stenoecious lifestyle, restricting them to cold habitats like glacial refugia (Asahina, 1954; Büsse, 2016; Büsse et al., 2012, 2015; Büsse & Ware, 2022; Davies, 1992; Mahato, 1993). *Epiophlebia laidlawi* is restricted to the Nepalese and Yünnanian refugia within the Himalayas of India, Tibet, and Bhutan, *E. superstes* is an endemic species of Japan, found in mountainous streams of the four main islands and one small island (Dōgo island) (Asahina, 1954, 1961a, 1961b; Hamada & Inoue, 1985), and *E. sinensis* is found within the Manchurian refuge with two localities within China and North Korea (Brockhaus & Hartmann, 2009; Büsse & Ware, 2022; Dorji, 2015; Fleck et al., 2013).

All three species possess very specific habitat requirements. In eastern Bhutan, abundance of *E. laidlawi* nymphs is negatively correlated with temperature and positively correlated with altitude; these nymphs reside within the headwaters of cold mountain streams with temperatures ranging from 11.5–16.3°C during the pre-monsoon season (April–May), and 8.5–11°C in the post-monsoon season (September–October); elevation ranges from 1300–3000 m throughout its range (Brockhaus & Hartmann, 2009; Nidup et al., 2020; Shah et al., 2012). Two individuals of *E. sinensis* were collected in the Changbaishan Mountains of China between 352–500 m, where yearly average temperature and precipitation are about ~ 2–3°C and 800 mm, respectively; winters can produce up to 2000 mm of snow (Chen et al., 2011; J. K. Li et al., 2012). A third specimen of *E. sinensis* was collected by Fleck et al. (2013), from Samjiyon County, Ryanggang province, North Korea, at 1380 m. *Epiophlebia superstes* is the most extensively studied species, with nymphs preferring streams with temperatures as low as 0.6°C in the winter and 10–22°C in the summer, with an extreme record of 23°C, with altitudes ranging from 1–2100 m (Asahina, 1948; Gose, 1953; Ishida et al., 1959; Okazawa, 1974; Tokuyama, 1992; Ubukata & Miyazaki, in press; Yamaura et al., 2009). Both *E. superstes* and *E. laidlawi* possess the longest development time of any odonate ranging from 5–8 years for both species (Dorji et al., 2020; Ozono et al., 2021).

Studies by Brockhaus & Hartmann (2009), and J. K. Li et al. (2012) suggest that the families Epiophlebiidae and the closely related extinct Stenophlebiidae belonged to an ‘archo-paleoarctic dragonfly fauna’, formed in the Jurassic at the breakup of Pangaea, with subsequent intermingling of oriental fauna in the Tertiary. However, phylogenetic and morphological analysis by Büsse et al. (2015) and Büsse (2016) suggest that the extant species of *Epiophlebia* constitute minor variants, and indeed genetic variation levels suggest a younger age of extant *Epiophlebia* than the Jurassic. Büsse et al. (2012) hypothesized that *Epiophlebia* might have possessed a continuous distribution within the last glacial maximum (LGM)(21 ka) allowing for a more recent genetic admixture to occur. Widespread cooling and the presence of a land bridge connecting Kyushu to Korea within the LGM might have allowed populations of *Epiophlebia* to be more widespread (Bintanja et al., 2005; Clark et al., 2009; Schmidt & Hertzberg, 2011; Tomita et al., 1975). Subsequent warming and sea level rise after the LGM might have resulted in *Epiophlebia* retreating to cooler and more elevated areas including foothill streams fed by groundwater, resulting in the disjunct populations currently seen. Furthermore, Büsse & Ware (2022) hypothesized other glacial refugia which have the climatic conditions suitable for harboring unsampled populations of current or new species of *Epiophlebia*.

The aim of this paper is to infer the historical range of *Epiophlebia* utilizing ecological niche modeling (ENM, or niche-based species distribution modeling) techniques.

ENM attempts to estimate the abiotic niche of a species by correlating occurrence and environmental data to generate an envelope of habitat suitability (Guisan & Thuiller, 2005; Guisan & Zimmerman, 2000; Zurell et al., 2020). Occurrence data is commonly obtained from natural history collections and citizen-science observations, while environmental data is derived from field stations or remote sensing in the form of climatic variables. Paleo-Ecological Niche Modeling (PaleoENM) provides the opportunity to estimate historical distributional patterns of a species by projecting modern day models onto paleoclimate layers, derived from a range of sources including global circulation models (GCM), ice sheet isotope data, or sedimentological proxies; such paleo-environmental layers can extend back into the Miocene (Brame & Stigall, 2014; Brown et al., 2018; Dudei & Stigall, 2010; Myers et al., 2015; Purcell & Stigall, 2021; Stigall, 2012). We combined verified occurrence records for all *Epiophlebia* species with averaged sets of environmental predictor variables to generate models for both modern-day and potential paleoenvironment distributions of the genus. We used these distribution models to not only infer unsampled areas of potentially suitable habitat for *Epiophlebia* but to determine if a continuous distribution of *Epiophlebia* between the Himalayas, Japan, and northern China existed within the LGM, suggesting a plausible route of gene flow.

## Methods

### Occurrence records

We acquired occurrence records of adult *Epiophlebia* species from the Global Biodiversity Information Facility (GBIF: [doi:10.15468/dl.fq95r7](https://doi.org/10.15468/dl.fq95r7)), as well as various published and unpublished datasets. We selected occurrences from GBIF possessing preserved museum samples and research grade observations, which include verified latitude and longitude coordinates, a photograph of the sighting, observation date, and at least  $\frac{2}{3}$  agreement on species identification by the community. We filtered occurrences by removing sightings from erroneous localities (middle of the ocean, locations of large museums). We acquired additional localities of *E. laidlawi* within India, Nepal, and Bhutan from Brockhaus & Hartmann (2009) and references cited therein, Dorji (2015), Tani & Miyatake (1979), Asahina (1961a, 1961b), and personal data from Büsse et al. (2012), as well as uncatalogued specimens housed within the Zoological Museum, Cambridge, UK, and the National Museum of Natural History, Smithsonian, USA. We acquired occurrence records of nymphs of *E. superstes*, focusing on maximum and minimum altitudes and temperate regions acquired by HU through a questionnaire survey sent out to more than 100 Japanese dragonfly researchers, as well as a substantial literature search. We also analyzed distribution maps of *E. superstes* nymphs and adults updated by TM's published and unpublished datasets. Details of both data collection

types are explained in detail within Ubukata & Miyazaki (in press). Finally, only two localities are known for *E. sinensis* within Eastern China and North Korea, which we acquired from J. K. Li et al. (2012) and Fleck et al. (2013). We opted not to include the locality for the type specimen of *E. diana* due to the misplacement of the specimen (Büsse & Ware, 2022), as well as the vagueness of the locality being collected by "Dr. David C. Graham in the mountainous regions of western Szechuan" (Needham, 1930).

We generated three datasets consisting of occurrences for *E. superstes* ( $n = 447$ ), *E. laidlawi* ( $n = 102$ ), and a combined dataset of all three species ( $n = 551$ ). Although qualitative data on *Epiophlebia* suggests all three species inhabit similar niches (high altitude, cold streams), an assumption of genus-level ENMs is niche similarity among all species, as the same environmental data are inputted into a singular model. As such, we generated species-level ENMs for *E. superstes* and *E. laidlawi* to support our approach and check for similarity in environmental responses compared to our combined model. We were unable to generate models for *E. sinensis* due to a very low sample size ( $n = 2$ ).

### Environmental data

We acquired averaged sets of environmental predictor variables for modeling consisting of purely bioclimatic variables. All analyses were conducted using the statistical programming language R v. 4.1.2 (R Core Team, 2021), and all layers are in a latitude/longitude coordinate system using WGS84 datum. We acquired environmental rasters at 2.5 arc-second resolution ( $\sim 5$  km at the equator) from the CHELSA climate database v2.1 (Karger et al., 2017, 2023). We downloaded the 'Anthropocene' bioclimatic dataset (1979–2013) consisting of 19 bioclimatic variables extrapolated from monthly minimum and maximum temperature, humidity, mean, and coefficient of variation of annual solar radiation. Variables follow Worldclim v2 (Fick & Hijmans, 2017). Although occurrence records for *Epiophlebia* species range from the past 100 years, we considered the broad patterns observed within these long-term datasets as sufficient to accurately represent the environmental conditions for the taxa sampled.

### Species distribution modeling

Before modeling, we processed our occurrences to account for sampling bias, delineated a study extent to sample background points, and omitted highly correlated environmental variables. We spatially thinned occurrences to the resolution of our environmental variables to reduce the effects of sampling bias and artificial clustering (Veloz, 2009) using the ENMtools package (Warren et al., 2010) (Table 1). Since *Epiophlebia* are highly restrictive in their habitat requirements, we chose a study extent to include potentially unsampled areas between Nepal and Japan yet excluding large



**Table 1.** Sample size of occurrence localities before and after spatial thinning, and maxent ENM settings for *Epiophlebia superstes*, *Epiophlebia laidlawi*, and combined model of all three species (*E. laidlawi*, *E. superstes*, *E. sinensis*). Settings shown are feature class (features). Statistics shown are mean validation AUC (AUC<sub>val</sub>), mean omission rates for 10 percentile training values (OR10), Akaike Information Criterion (AICc), and delta Akaike Information Criterion (delta.AICc), and number of non-zero coefficients (ncoef).

Species	Raw occurrences	Thinned occurrences	Features	Regularization	AUC <sub>val</sub>	AICc	delta.AICc	OR10	ncoef
<i>Epiophlebia superstes</i>	447	134	LQH	3	0.79	2653.97	0.00	0.13	11
<i>Epiophlebia laidlawi</i>	102	38	LQ	1	0.97	651.91	0.00	0.12	10
Combined Model	551	174	LQH	2	0.92	3628.27	0.00	0.12	35

areas outside the species’ dispersal limitations (Peterson & Soberón, 2012), defined as point buffers around all localities buffered by 5 degrees (approx. 500 km at equator) (Fig. 1). Within this extent, we randomly sampled 50,000 background points for modeling and extracted their environmental values. We used these values to calculate correlations between variables using the ‘vifcor’ and ‘vifstep’ functions in the ‘usdm’ package (Naimi, 2017) and filtered out variables with correlation coefficients higher than 0.7 and a VIF threshold of 10. Finally, we removed bioclimatic variables 8, 9, 18, 19 after visual inspection of interpolation discontinuities (Booth, 2022). Although such spatial artefacts were

minor within our initial study extent, we observed major breaks of climate smoothing when we extrapolated our model to a larger spatial extent which included glacial refugia hypothesized by Büsse & Ware (2022).

To model the distribution of *Epiophlebia*, we used the presence-background algorithm Maxent v3.4.4 (Phillips et al., 2017), which remains one of the top-performing models for fitting ENMs with background data (Valavi et al., 2021). We used the R Package ‘ENMeval’ 2.0.0 (Kass et al., 2021) for model building, parameterization, evaluation with different complexity settings, and reporting of results. Since our occurrences varied greatly in space, we partitioned our data using the ‘leave-one-

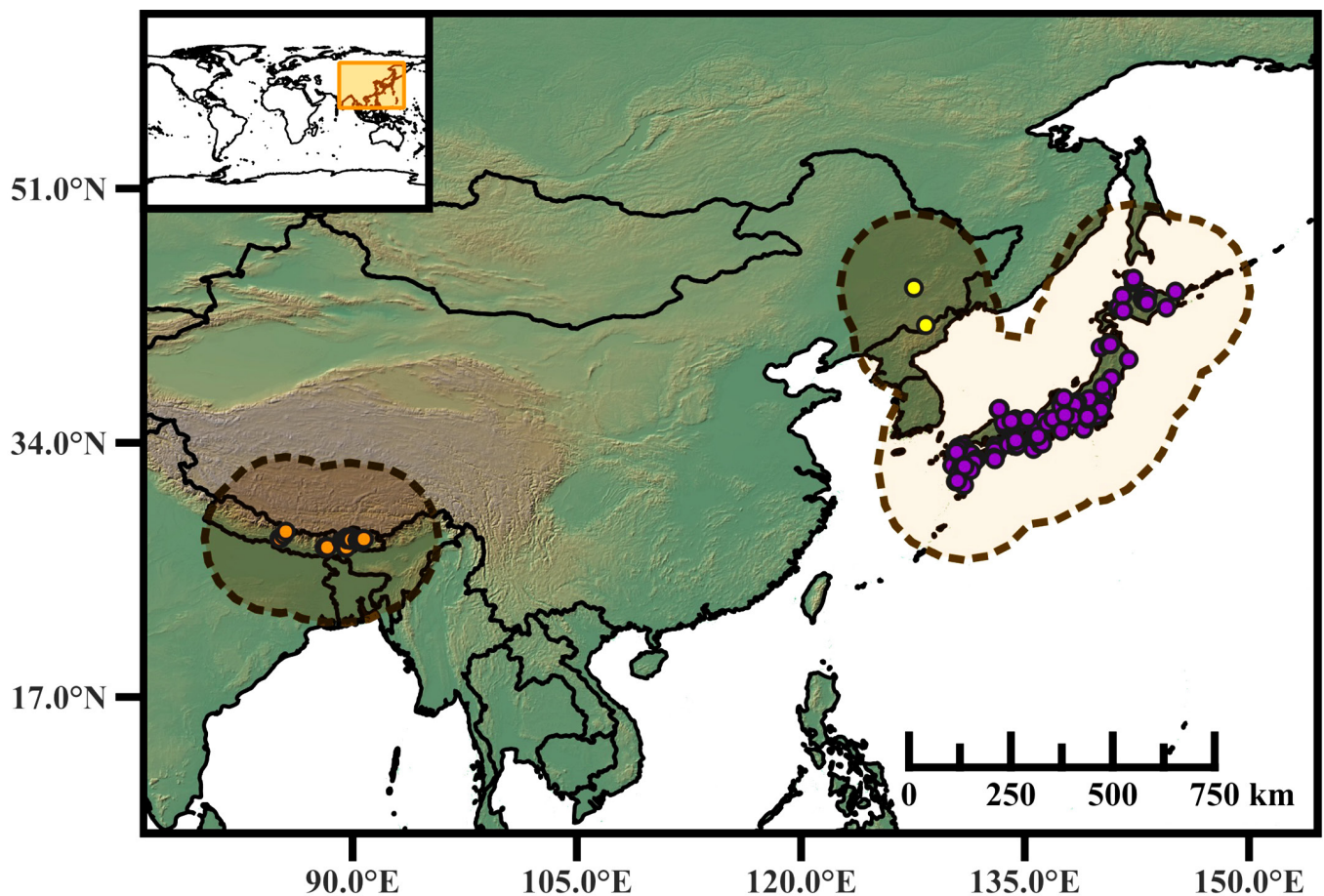


**Figure 1.** Range of occurrences for *Epiophlebia* throughout Asia. Dashed lines indicate our study extent defined as point buffers around all localities buffered by 5 degrees (~ 500 km at the equator). Purple points are previous localities for *E. superstes*, yellow points are *E. sinensis* and orange points are *E. laidlawi*.



out' strategy (referred to as "jackknife" in 'ENMeval') to fully encapsulate the climatic ranges of each species, and each occurrence. We clamped our models by omitting ranges of environmental data which fall outside of our training data, to prevent projection of our model to non-analogue climates. All final models were fitted to the full dataset.

We tuned model complexity to find optimal settings (Radosavljevic & Anderson, 2014; Warren & Seifert, 2011). For tuning, in order of increasing complexity, we chose the feature classes linear (L), quadratic (Q), and hinge (H), as well as regularization multipliers one through five (higher numbers penalize complexity more).

We assessed our model using averages of threshold-dependent (omission rate) and threshold-independent (AUC) discrimination performance metrics calculated on withheld validation data, (Warren & Seifert, 2011). We assessed the 10-percentile omission rate, which sets a threshold as the lowest suitability value for occurrences after removing the lowest 10% suitability values (Kass et al., 2021; Radosavljevic & Anderson, 2014). Validation AUC is a measure of discrimination accuracy that can be used to make relative comparisons between ENMs with different settings fit on the same data (Lobo et al., 2008; Radosavljevic & Anderson, 2014). If a series of models possessed near-identical AUC values and 10-percentile omission rates, we chose the simplest model, or the one with the fewest non-zero lambda values (model coefficients).

To investigate model behavior, we examined predictor variable importance values and marginal response to suitability. Permutation importance is calculated by randomly permuting the values of all variables but one, building a new model, then calculating the difference between each model's training AUC and that of the global model (Phillips, 2021). Marginal response curves show the modeled relationship of each variable individually with the occurrence data when all other variables are held constant and are affected by the complexity of the model settings (Phillips et al., 2017).

We made habitat suitability predictions for *Epiophlebia* using our 'Anthropocene' environmental predictor variables. Predictions were estimated using a new study extent, generated as a bounding box encapsulating all the glacial refugia hypothesized by Büsse & Ware (2022). We chose this new study extent for our predictions to estimate potential routes of dispersal of *Epiophlebia* during the LGM, as well as to identify potentially new under-sampled refugia hypothesized by Büsse & Ware (2022). Maxent raw predictions were transformed to a scale of 0–1 to approximate probability of occurrence using the 'cloglog' transformation (now referred to as our continuous prediction) (Phillips et al., 2017). We also generated a threshold prediction, calculated from the 10-percentile omission rate from our model evaluation. To estimate habitat suitability of *Epiophlebia* within the geologic past, we generated predictions using environmental predictor variables from

the PaleoClim dataset (Brown et al., 2018). We generated predictions within eight distinct time periods: late-Holocene (Meghalayan: 0.3–4.2 ka), mid-Holocene (Northgrippian: 4.2–8.326 ka), early Holocene (Greenlandian: 8.326–11.7 ka), Younger Dryas Stadial (11.7–12.9 ka), Bølling-Allerød (12.9–14.7 ka), Heinrich Stadial (14.7–17.0 ka), the Last Glacial Maximum (21 ka), and the Last Interglacial (130 ka), generated from the CHELSA database.

Finally, we calculated multivariate similarity surface (MESS) maps (Elith et al., 2010) to detect areas with novel climatic conditions between our modern-day and paleoclimate variables. MESS calculates environmental similarity by extrapolation of environmental values from our occurrence points to different climate conditions. In the case of our data, we calibrated our occurrence points by extracting environmental values from our 'Anthropocene' variables. We then calculated similarity between our occurrences and each of our paleoclimate layers. Negative MESS values indicate geographic regions of our paleoclimate variables falling outside our 'Anthropocene' variables (i.e., extrapolation), while positive values indicate regions which fall within our 'Anthropocene' variables (interpolation).

## Results

Optimal model settings for *Epiophlebia* exhibited robust results based on a 10-percentile omission rate and mean validation AUC. Based on the results of the collinearity analysis, we used the following six predictor variables to build all models: temperature seasonality (bio04), maximum temperature of the warmest month (bio05), mean diurnal range (bio02), precipitation of the driest month (bio14), precipitation of the wettest month (bio13), and precipitation seasonality (bio15). Our optimal model was complex, with linear, quadratic, and hinge feature classes and a regularization multiplier of 2 (lower complexity penalty). Our mean validation AUC was very high (0.92), and a 10% omission rate that was low (0.12) relative to its expected value of 0.1. Furthermore, the optimal model possessed an AICc of 3628.27, a delta AICc of 0, and 32 non-zero lambda values, indicating a slight overfitting of model prediction. Individual models of *E. superstes* and *E. laidlawi* exhibited similar robust results (Table 1).

Temperature seasonality (bio04) possessed the highest variable importance (46%), followed by maximum temperature of the warmest month (bio05) (30%), mean diurnal range (bio02) (14%), precipitation of the driest month (bio14) (6%), while precipitation of the wettest month (bio13), and precipitation seasonality (bio15) possessed < 2% (Supplementary Fig. S1). Temperature seasonality (bio04), mean diurnal range (bio02), maximum temperature of the warmest month (bio05), and precipitation seasonality (bio15) expressed quadratic relationships with suitability. Precipitation of the driest month (bio14) also expressed a quadratic/lin-

ear relationship but with jagged optimal ranges mostly likely due to the disjunct spread of occurrence points. To preserve significant digits, bioclimatic-based temperature variables are multiplied by 10, while temperature seasonality is multiplied by 100 (O'Donnell, 2012). As such, we report the absolute values of temperature-related variables in relation to suitability. Precipitation of the wettest month (bio13) expressed a positive linear relationship with suitability, saturating at 750 mm (Supplementary Fig. S1). Suitability was highest at 50–80°C for temperature seasonality (bio04) (calculated as the standard deviation of average monthly temperature  $\times$  100), 7.5°C for mean diurnal range (bio02), 20–30°C for maximum temperature of the warmest month (bio05), 10 mm and 260 mm for precipitation of the driest month (bio14), > 750 mm for precipitation of the wettest month (bio13), and 50 mm for precipitation seasonality (bio15).

Individual models for *E. superstes* and *E. laidlawi* exhibited similar variable importance compared to our combined model, but in some cases, response curves of *E. superstes* and *E. laidlawi* exhibited opposite response curves (Supplemental Figs S1–3). Within all three models, maximum temperature of the warmest month (bio05) exhibited high variable importance. However, *E. laidlawi* exhibited a quadratic relationship with suitability, while *E. superstes* exhibited a negative linear relationship; the combined model also exhibited a quadratic relationship. Precipitation of the driest month (bio14) was also shared among our three models, however *E. laidlawi* expressed a negative linear relationship, *E. superstes* exhibited a positive linear relationship, with suitability increasing with lower rainfall, and the combined model exhibited a jagged quadratic relationship. Finally, precipitation seasonality (bio15) expressed a quadratic relationship within *E. laidlawi* and our combined model, but a negative linear relationship in the case of higher precipitation seasonality within *E. superstes*. Some variables were shared between individual species and our combined model such as temperature seasonality (bio04) which expressed a negative linear relationship within *E. superstes* but a quadratic relationship within our combined model. Mean diurnal range (bio02) was shared between *E. laidlawi* and our combined model but expressed a negative linear and quadratic relationship, respectively.

Predictions over the study extent for our 'Anthropocene' environmental variables revealed areas of high suitability across the Himalayas (Nepal, Tibet, Bhutan, northern India, and Myanmar), eastern coastal China (Fujian province), central China (Sichuan province), and all the Japanese Islands—these regions range between 1200–3000 m, except in Japan and North Korea, consistent with previous sightings and the biology of *Epiophlebia*. We also observed sparse areas of high suitability within coastal South Korea and the Kamchatka peninsula of Russia. However, suitability was low within North Korea and northeast China, where sightings of *E. sinensis* have occurred (Fig. 2A). Areas of high suit-

ability partially overlap with hypothesized refugia of *Epiophlebia* from Büsse & Ware (2022), particularly within the areas of near Taiwan (Sino-Pacific refuge), northern Vietnam, Laos, and Myanmar (Yünnanian refuge), Nepal and Bhutan (Nepalese refuge). Such areas of suitability from our continuous predictions are congruent with threshold maps generated from our 10% omission rates, however coastal South Korea, the Kamchatka peninsula, and southwestern Hokkaido (where *E. superstes* inhabits) were classified as 'unsuitable' (Fig. 2B).

Predictions generated from our paleoclimate variables demonstrated variability in suitability over our time intervals compared to our modern-day 'Anthropocene' variables, suggesting that the occupancy of the various glacial refugia differed since the LGM (Fig. 3). Suitability shifted southward within the Holocene (0.3–12.9 ka) into Myanmar, eastern India, and Laos (Yünnanian refuge) (Figs 3B–E). Within the Bølling-Allerød (12.9–14.7ka), suitability within the Yünnanian refuge began to decrease, but suitability extended eastward off the coast of China due to increased glaciation, recession of the ocean, and subsequent expansion of landmass into the East China Sea (Fig. 3F). Also, a land bridge was observed within Hokkaido, connecting Northern Japan with Russia, suggesting the beginning of the Würm glaciation (Clark et al., 2009); however, suitability was low within this region. Expansion of landmass continued within the Heinrich Stadial (14.7–17.0 ka), creating a land bridge between Coastal China, Taiwan, the Korean Peninsula, and the Yellow Sea with suitability being high within these areas, suggesting an increased importance of the Sino-Pacific refuge and reduced importance of the Sino-Tibetan refuge (Fig. 3G). Within the LGM, a complete land bridge formed, connecting northwestern coastal Japan (Northern Kyushu) to the southernmost point of South Korea with suitability being high within this area (Fig. 3H). However, suitability was significantly lower throughout central China and most of the mountainous or northern areas of Japan.

Threshold (10-percentile omission rate) predictions revealed slightly different patterns to our continuous predictions, with areas considered suitable being considerably larger across the time periods sampled (Fig. 4). Areas considered suitable remained relatively constant until the Bølling-Allerød (12.9–14.7 ka), overlapping with the threshold prediction of our 'Anthropocene' variables; the exception being the Kamchatka refuge becoming more suitable along with eastern India, Myanmar, Laos, northern Vietnam, the land bridge connecting Coastal China, Taiwan, the Korean Peninsula, and the Yellow Sea (Figs 4B–F). Within the Heinrich Stadial (14.7–17.0 ka), areas considered suitable decreased within central China, as well as Kamchatka, suggesting that the Kamchatka refuge possessed high importance within the historic past but not recently (Fig. 4G). Within the LGM, suitable areas encapsulated most of coastal China while Kamchatka was completely unsuitable. Suitability expanded eastward back into

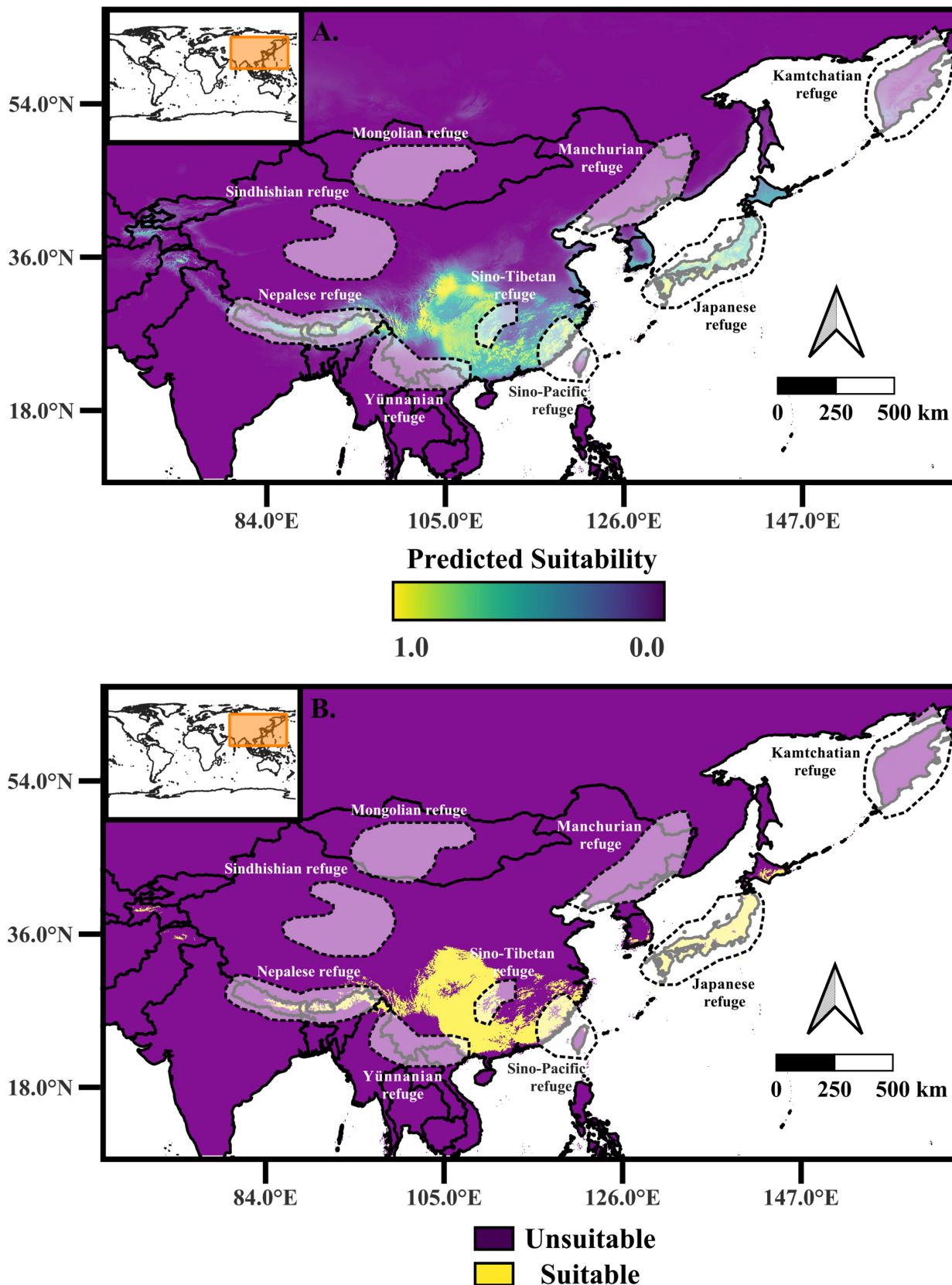


**Figure 2.** Maxent prediction for *Epiophlebia* projected using our ‘Anthropocene variables’, with hypothesized refugia for *Epiophlebia* adapted from Büsse & Ware (2022). Predictions were derived from the optimal model using the criterion of  $AUC_{test}$  values being the highest, and 10% omission rate being the lowest. Predictions were transformed using the ‘cloglog’ function on Maxent v3.4.4 (Phillips et al., 2017), in which raw values are converted to a range of 0–1 to approximate a probability of occurrence (A). We also generated a threshold prediction, calculated from the 10-percentile omission rate from our model evaluation (B). Brighter colors (yellow, green, blue) indicate areas of higher suitability (higher probability of occurrence), while darker colors (violet) indicate areas of lower suitability (lower probability of occurrence). For threshold predictions bright colors indicate areas deemed ‘suitable’ while colder colors indicate areas deemed ‘unsuitable’. Orange points are our thinned dataset of *Epiophlebia* occurrences.



Central China (Sino-Tibetan refuge) with pockets of suitable habitat reaching as far west as Pakistan, Afghanistan, Tajikistan, Kyrgyzstan, Kazakhstan, and Uzbekistan (Fig. 4H). Overall, suitability within the LGM reveals a potential continuous route of genetic admixture that is lost within modern-day disjunct populations (Fig. 4H). During the Last Glacial Maximum, and the Last Interglacial (130 ka), suitable habitat for *Epiophlebia* expanded south to Thailand, and southern Vietnam (Fig. 4I).

MESS analyses indicated that most of the study area presented novel paleoclimate conditions throughout our time intervals (Fig. 5). Climatic similarity within our modern-day 'Anthropocene' variables were highest within central and eastern coastal China, Taiwan, Korea, Japan, Sakhalin, and the Russian coastal area on the opposite bank, Kamchatka, eastern India, Myanmar, and Laos producing similar results from our suitability predictions (Fig. 5A). However, similar climatic conditions within eastern China (Fujian province) shifted eastward and decreased going backward within our time intervals, resulting in extremely similar climatic conditions within the land bridge connecting southern Japan with coastal Korea, eastern China and Taiwan within the LGM (Fig. 4H).

## Discussion

### *Environmental preferences of Epiophlebia*

Within our model, it appears that monthly temperature extremes and seasonality are the main variables driving suitability, suggesting that large-scale fluctuations in temperature better explain distributions for *Epiophlebia*. Variables which possessed high importance within our models were recovered with the same importance within ENMs of both Nearctic and Palearctic species (Abbott et al., 2022; Kalkman et al., 2022). The four most important variables exhibited quadratic relationships with suitability, however some response curves were jagged, which can be explained by the disparate localities of *Epiophlebia*, prompting the model to encapsulate a large spectrum of environmental gradients for extrapolation of suitability.

It is interesting that both *E. superstes* and *E. laidlawi*, despite the substantial geographic gap between their ranges, exhibited similar importance in bioclimatic variables. Even more interesting is the contradictory patterns within their responses to such bioclimatic variables. Since genus-level maxent models assume similar niches of all species included, the argument can

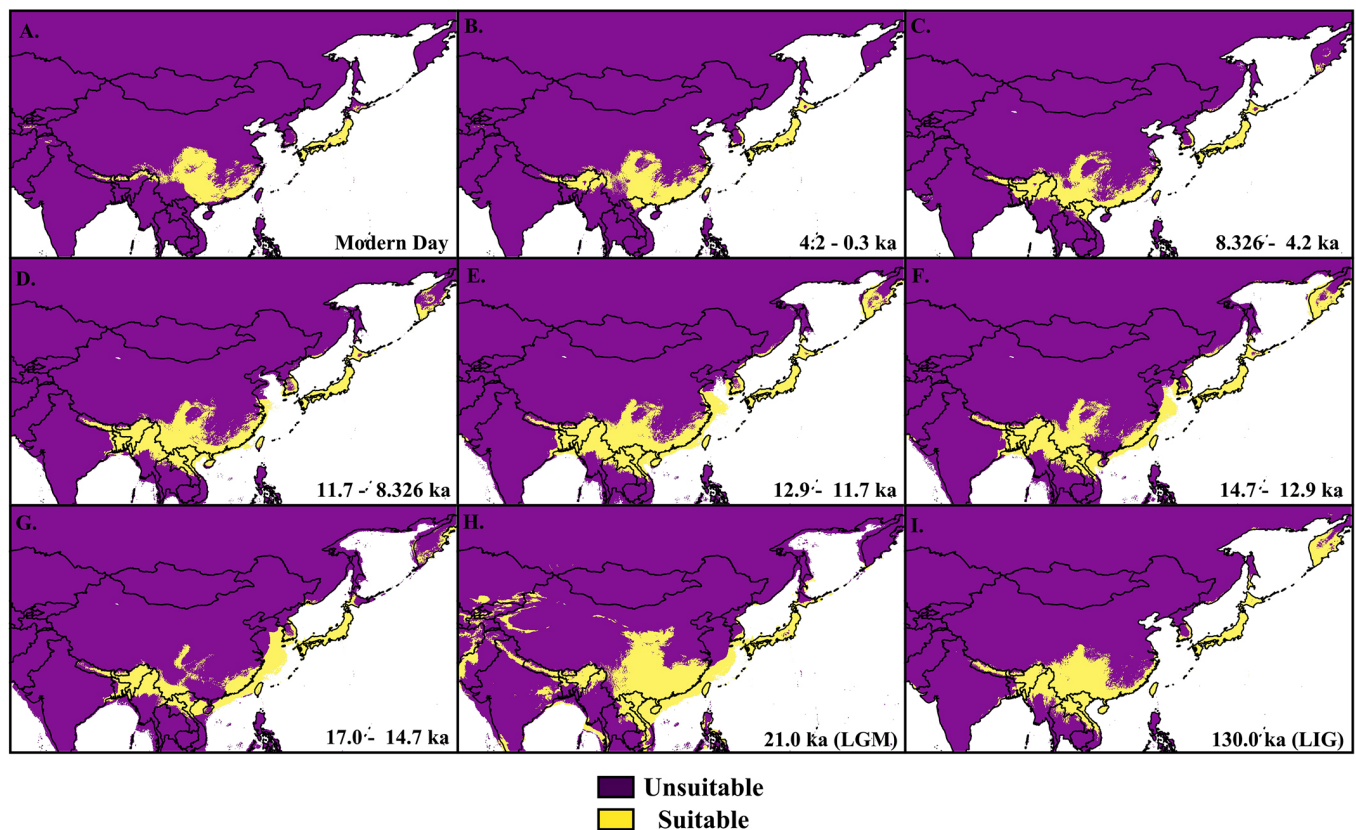


**Figure 3.** Maxent predictions for *Epiophlebia* projected to the modern day using our 'Anthropocene variables' (A) and the late-Holocene (Meghalayan: 0.3–4.2 ka) (B), mid-Holocene (Northgrippian: 4.2–8.326 ka) (C), early Holocene (Greenlandian: 8.326–11.7 ka) (D), Younger Dryas Stadial (11.7–12.9 ka) (E), Bølling-Allerød (12.9–14.7 ka) (F), Heinrich Stadial (14.7–17.0 ka) (G) from our PaleoClim variables, and the Last Glacial Maximum (LGM) (21 ka) (H) and Last Interglacial (LIG) (130 ka) (I) generated from the CHELSA database (H) (Brown et al., 2018). Predictions were derived from the optimal model using the criterion of  $AUC_{test}$  values being the highest, and 10% omission rate being the lowest. Predictions were transformed using the 'cloglog' function in Maxent v3.4.4 (Phillips et al., 2017), in which raw values are converted to a range of 0–1 to approximate a probability of occurrence. Brighter colors (yellow, green, blue) indicate areas of higher suitability (higher probability of occurrence), while darker colors (violet) indicate areas of lower suitability (lower probability of occurrence).

be made that our combined model portrays a biased picture of the distribution of *Epiophlebia* due to differing species-level response curves. However, we justify combining all three species as the importance of climatic variables did not differ significantly among *E. superstes* and *E. laidlawi*, suggesting such variables may possess evolutionary and phylogenetic importance as both species are sister taxa (Büsse & Ware, 2022).

Optimal suitability for temperature seasonality (standard deviation of the mean monthly temperature) was highest at 5°C suggesting that *Epiophlebia* exhibits a narrow threshold to temperature fluctuation. Since both *E. laidlawi* and *E. superstes* prefer to inhabit the headwaters of mountainous streams (Asahina, 1961a, 1961b; Brockhaus & Hartmann, 2009), we hypothesize that *Epiophlebia* are highly susceptible to large scale temperature perturbations due to the species-level adaptation to cool mesic refugia on the tops of the Himalayas and throughout Japan. Although annual average temperature for *E. sinensis* is about 2–3°C, we accredit the discrepancy of temperature differences among our species due to the large-scale extrapolation of our model to encapsulate the environmental preferences of all

three species. Optimal suitability for mean temperature of the warmest month was 20–30°C which supports the average temperature preferences for *E. laidlawi* (Brockhaus & Hartmann, 2009).

In the case of *E. superstes*, the optimal suitability for average temperature of the warmest month is 15.8–27.2°C (Ubukata and Miyazaki, *in press*), slightly lower than *E. laidlawi*. Utilizing regression data derived from altitude and the Japan Meteorological Society's Automated Meteorological Data Acquisition System (AMeDAS), Ubukata & Miyazaki (*in press*) explored the relationship between temperature and distribution of *E. superstes*. In terms of larval data, *E. superstes* can live in torrents with average annual temperatures of 2.4–17.2°C, average temperatures of the coldest and warmest months of -9.5–7.5°C and 15.8–27.2°C, respectively, and average daily minimum temperatures of the coldest month from -17.7–3.0°C. In terms of adult data, the minimum temperatures were estimated for a torrent (780 m) in Hokkaido as follows: average annual temperature is 1.8°C, average temperature of the coldest and warmest months is -11.5 and 15.8°C, respectively (coinciding with the Honshu highlands, the highest altitude records of

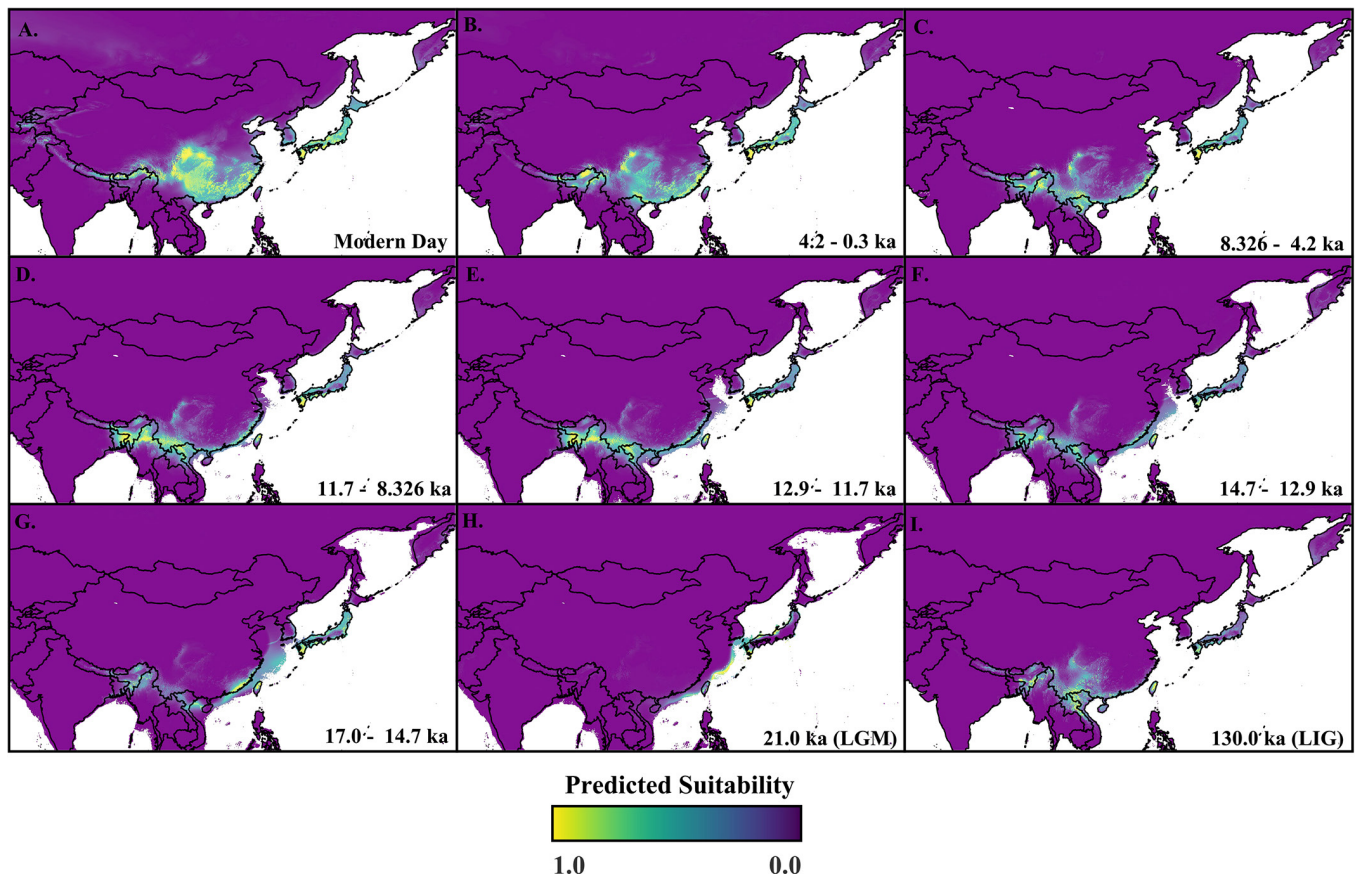


**Figure 4.** Thresholded maxent predictions for *Epiophlebia* projected to the modern day using our ‘Anthropocene variables’ (A), and the late-Holocene (Meghalayan: 0.3–4.2 ka) (B), mid-Holocene (Northgrippian: 4.2–8.326 ka) (C), early Holocene (Greenlandian: 8.326–11.7 ka) (D), Younger Dryas Stadial (11.7–12.9 ka) (E), Bølling-Allerød (12.9–14.7 ka) (F), Heinrich Stadial (14.7–17.0 ka) (G) from our PaleoClim variables, and the Last Glacial Maximum (LGM) (21 ka) (H) and Last Interglacial (LIG) (130 ka) (I) generated from the CHELSA database (H) (Brown et al., 2018). Predictions were derived from the optimal model using the criterion of  $AUC_{test}$  values being the highest, and 10% omission rate being the lowest. Threshold predictions were calculated from the 10-percentile omission rate from our model evaluation. Bright colors (yellow) indicate areas deemed ‘suitable’ while colder colors (violet) indicate areas deemed ‘unsuitable’.



larvae within Japan), and average daily minimum temperature of the coldest month is -17.1°C. If adult and larval data are combined, the lowest limits of average annual and coldest month temperature ranges are lowered by the collection record in Hokkaido. Overall, it appears that *E. superstes* can live within warmer climates (especially in the summer) than its continental conspecifics.

Although precipitation seasonality (bio15), and precipitation of the driest and wettest months (bio13 and 14) possessed minimal importance within model building, we still consider such variables vital in determining distribution of the genus due to the disparate elevational and resultant rainfall regimes present within each species' range. Previous ENM work on *E. laidlawi* in the context of future climate change demonstrated that annual precipitation possesses high importance within model building (Dorji et al., 2020; Shah et al., 2012). Localities of *E. sinensis* within the Changbai-shan Mountains experience roughly 2000 mm of snow, short hot summers, with mean annual precipitation of

800 mm (J. K. Li et al., 2012). In the case of *E. superstes*, the geologic features of Japan are particularly interesting, as variability of rainfall on both sides of Japan have allowed the species to reside nearly at sea level.

Comparing the estimated summer water temperatures of rivers of Japan (Amano & Mochizuki, 2011) to known occurrences of *E. superstes*, we find that records of the species are absent or rare when temperatures exceed 30°C. However, when summer water temperatures are below 25°C, there are records of *E. superstes* even at low-altitude mountain streams (1–30 m) near the coast (e.g., the Owase region of Mie Prefecture and the northeastern corner of Toyama Prefecture; Ishida et al. [1959], Futahashi et al. [2004]). A common characteristic of these areas is that annual precipitation exceeds 3000 mm (see Japan Meteorological Agency Website: [data.jma.go.jp/stats/etrn/view/atlas/docs2020/png\\_small/prec/precipitation\\_13.png](http://data.jma.go.jp/stats/etrn/view/atlas/docs2020/png_small/prec/precipitation_13.png)), most likely due to humid oceanic winds hitting high elevation mountains (> 1000 m) supplying cool spring water throughout the year.

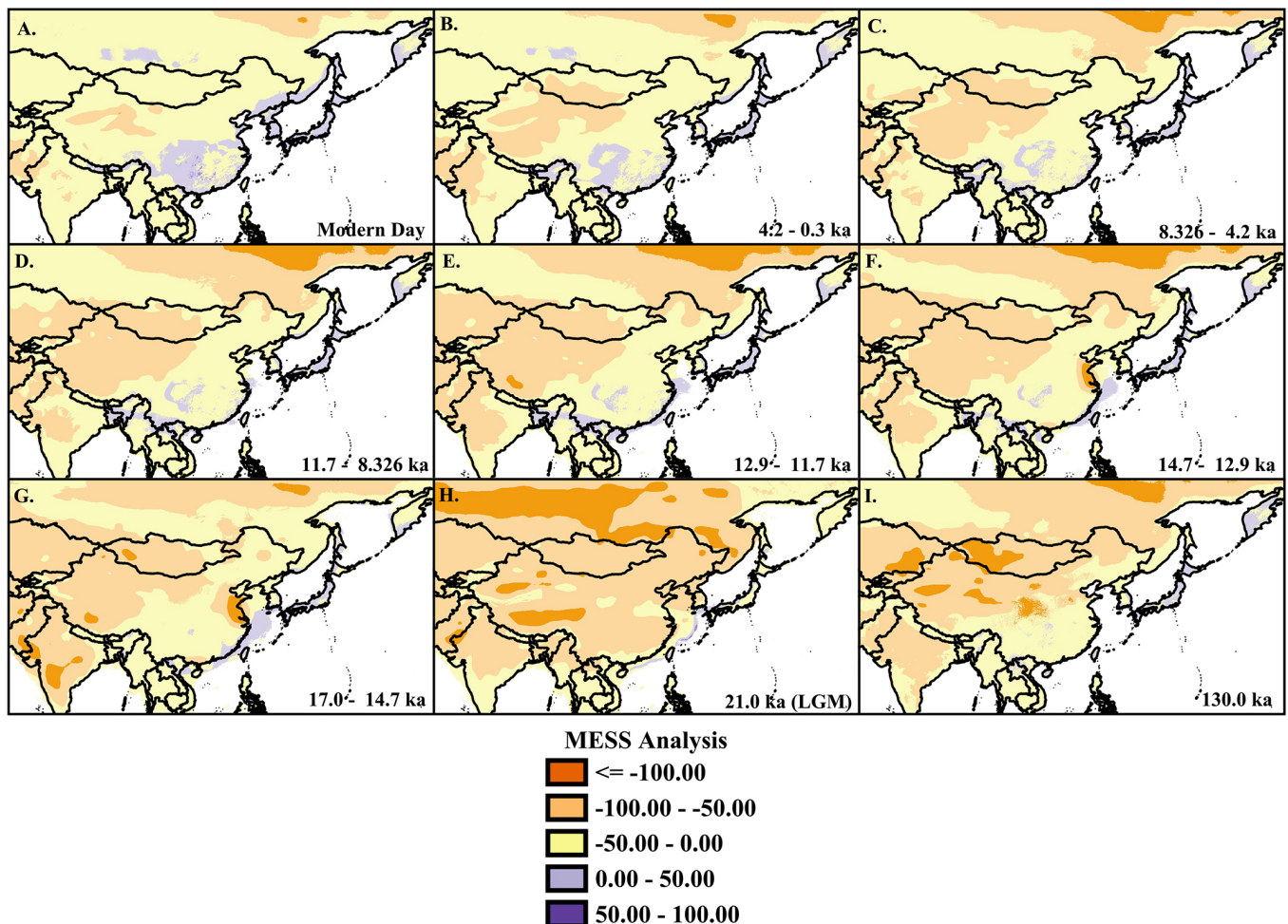


**Figure 5.** Multivariate environmental similarity surface (MESS) analysis described in Elith et al. (2010) and calculated using the ‘ENMeval’ package in R using our ‘Anthropocene’ variables (A), late-Holocene (Meghalayan: 0.3–4.2 ka) (B), mid-Holocene (Northgrippian: 4.2–8.326 ka) (C), early Holocene (Greenlandian: 8.326–11.7 ka) (D), Younger Dryas Stadial (11.7–12.9 ka) (E), Bølling-Allerød (12.9–14.7 ka) (F), Heinrich Stadial (14.7–17.0 ka) (G) from our PaleoClim variables, and the Last Glacial Maximum (LGM) (21 ka) (H) and Last Interglacial (LIG) (130 ka) (I) generated from the CHELSA database (H) (Brown et al., 2018). Negative scores (shown in orange) indicate novel climate conditions (i.e., bioclimatic values that fall outside the range of the ‘Anthropocene’ variables for each Paleoclim time interval). Positive scores (shown in purple) indicate climate conditions similar to our ‘Anthropocene’ variables.



The Japanese archipelago consists of the long and narrow island of Honshu and three large islands connected to it across straits. Honshu has a maximum altitude of 3776 m (Mt. Fuji), with the other three islands possessing mountains ranging from 1900–2200 m in altitude. Except for some coastal plains, all Japanese mountains are adjacent to the ocean, some of which possess steep slopes covered in temperate forests (subarctic forest in the north). The elevational gradients of such mountains with abundant rainfall have resulted in cool water (< 22°C), allowing larvae of *E. superstes* to inhabit mountain streams even at lower elevation. One such example is Mt. Inaodake, in the southernmost part of Kyushu's Osumi Peninsula, which is 959 m in elevation, and 2–3 km from the coast where imagines *E. superstes* were collected at 427 m on the northern slope (Matsuhira, 1996); the average annual precipitation at the nearest AMeDAS point (Tashiro) is 2880 mm.

Except for Hokkaido, Japan experiences abundant rainfall during the rainy season from June to July. Since Japan is located between the Pacific Ocean to the southeast and the Sea of Japan to the northwest, differences in rainfall patterns occur along both sides of the archipelago. On the Pacific side of southern Honshu, Shikoku, and Kyushu, summer breezes carry moisture resulting in abundant rainfall. During the winter, northwest monsoons bring heavy snowfall to the mountains closer to the Sea of Japan. Such deep snowfall can be seen even in the early spring, where it melts, supplying rivers and tributaries with cold water. Such complex patterns in precipitation allow constant replenishment of groundwater, permitting *E. superstes* to inhabit both mountain and coastal torrents along the Pacific and the Sea of Japan sides of Japan.

Within mainland Japan (Hokkaido, Honshu, Kyushu, and Shikoku), Chiba Prefecture is the only prefecture where *E. superstes* is absent (highest elevation 408 m). Ubukata & Miyazaki (in press) analyzed the factors contributing to the absence as follows. Although climate warming since the last ice age has caused a rise of about 6°C by the 20<sup>th</sup> century, temperatures in the lowlands of Chiba Prefecture remain within the habitable mean air temperature range for *E. superstes*. Notwithstanding that this region faces the ocean, there are no mountains exceeding 500 m, so there is not so much (less than 2000 mm) annual precipitation, making it difficult to provide a stable supply of cool (22°C or less) running water to mountain streams. This results in the estimated summer water temperature of this area exceeding 30°C.

### Modern day predictions of *Epiophlebia*

Our models support the findings of Büsse & Ware (2022), in which we estimate high suitability for *Epiophlebia* within the Japanese, Nepalese, and Yunnanian refugia, overlapping previous records of *E. superstes* and *E. laidlawi* respectively. Furthermore, Büsse & Ware (2022) hypothesized that due to the presence

of other glacial refugia throughout Asia (Lattin, 1967), other *Epiophlebia* habitats may exist within the Sino-Pacific refuge, the Sindhianian refuge (northwest China), the Mongolian refuge, as well as the Manchurian and Kamchatka refugia (see Büsse & Ware [2022]). Our results partially support the hypothesis of Büsse & Ware (2022) in which suitability for *Epiophlebia* was high within the Sino-Pacific refuge off the coast of Taiwan and eastern China, and the Sindhianian refuge bordering eastern India, Myanmar, and Vietnam (Fig. 2). Furthermore, we recorded large swaths of high suitability within central China as well as the Sino-Tibetan refuge, elucidating potentially undersampled habitats for *Epiophlebia* (Fig. 2). Interestingly, the type specimen for the recently demoted *E. diana* was collected within the western Sichuan mountains (Carle, 2012; Needham, 1930). Designation of *E. diana* to *E. laidlawi* supports our findings by pushing the range of *Epiophlebia* within central China, increasing the support of suitable habitat eastward. However more occurrence records are required to verify as the type locality for *E. diana* was too vague to incorporate within or analysis.

Predictions of *Epiophlebia* also partially refute the hypotheses of Büsse & Ware (2022), in which suitability was low within the Sindhianian, Mongolian, Manchurian, and Kamchatka refugia (Fig. 2). Although our continuous predictions suggest intermediate suitability within Northern Russia (Kamchatka refuge) and coastal North Korea (Manchurian refuge), our threshold predictions classify these areas as unsuitable, most likely due the stringency of our 10% threshold. However, the Manchurian and Kamchatka refugia are climatically similar to the Japanese, Nepalese, and Yunnanian refugia (Fig. 5A), and individuals of *E. sinensis* were recorded at 500 m within North Korea (Fleck et al., 2013; J. K. Li et al., 2012). Furthermore, it is unlikely that Kamchatka refugia harbors *Epiophlebia*, as multiple generations of populations would be required to travel north along the coast of Okhotsk, passing through the base of the Kamchatka Peninsula even if the distance between the tip of the Kamchatka Peninsula and its base is somewhat shortened due to the sea level fall in the LGM.

We therefore hypothesize that glacial refugia may still harbor *Epiophlebia* but will require sampling to verify. In the case of the Sindhianian and Mongolian refugia we hypothesize that such areas may not possess the environmental requirements of *Epiophlebia* due to their strict winter and summer temperature ranges (Brockhaus & Hartmann, 2009). Our MESS analysis supports this claim, as the Sindhianian and Mongolian refugia possess very dissimilar climates compared to the Japanese, Nepalese and Yunnanian refugia.

### Paleoclimate predictions of *Epiophlebia*

Our paleoclimate predictions revealed the potential for a continuous distribution of *Epiophlebia* between the Himalayas, Japan, and northern China within the LGM, suggesting a continuous route of gene flow among the

disparate current populations. The connection between Japan, mainland China, and the Himalayas within the LGM has been well documented, referred to as the Sino-Japanese floristic region (Büsse et al., 2012; Ikeda, 1998). Our models suggest that a continuous route of dispersal was plausible. Although our continuous predictions restrict suitability from Japan to coastal China down to Taiwan, our threshold predictions reveal large swaths of suitability within central China as well as the Himalayas and parts of western India (Figs 3, 4). Differences of both prediction types can be accredited to the geographic separation of all three species included in our model, as made evident by our MESS analysis display large variation in climate since the LGM. Our continuous predictions emphasize the highest suitable areas within our study extent, while our thresholded maps flatten our predictions based on omission, correcting any uncertainty. As such, we discuss two distinct dispersal scenarios of *Epiophlebia* since the LGM, based on both prediction types (Fig. 6).

According to our continuous predictions, the first hypothesis is that *Epiophlebia* possessed a continuous distribution from Japan to coastal China, but climatic conditions allowed for expansion as the Japanese land bridge closed. Starting in the Heinrich Stadial (17.0–14.7 ka), suitability within the Sino-Pacific, Sino-Tibetan, Yünnanian, and Nepalese refugia increased, potentially acting as a stepping stone for dispersal for *Epiophlebia* westward. Concurrently, the coastal regions connecting Japan to Korea and China were closing, isolating populations of *Epiophlebia* still in Japan. Suitability shifted northward within the Younger Dryas Stadial (11.7–12.9 ka), expanding into Central China (Sichuan and Fujian provinces) throughout the rest of the Holocene, resulting in the modern-day distribution (Fig. 6A). According to our threshold predictions, the second hypothesis is that *Epiophlebia* possessed a continuous distribution throughout the Himalayas to Japan but became isolated due to the closing of the land bridge connecting Japan to the rest of Asia. Throughout the rest of the Holocene, suitability decreased resulting in the occupancy of *Epiophlebia* to the modern-day glacial refugia (Fig. 6B). Our MESS analysis seems to support the former of these two hypotheses in which climate similarity is highest along the coasts of Japan, Korea, and China within the LGM, and decreases over time as climate similarity increases within central China until the modern-day. Regardless of these two hypotheses, it seems that the glacial refugia of Asia acted as retreats for *Epiophlebia* during times of warming, resulting in the current disjunct populations currently seen.

An interesting observation within our predictions is the ephemeral use of the Manchurian and Kamchatka glacial refugia since the LGM. According to our threshold predictions, both glacial refugia possessed suitable habitat from 4.2–17.0 ka, suggesting they acted as potential routes of dispersal in the past, but have since become obsolete. However, distances between adjacent islands in the Kuril Islands which connect North-

ern Japan (Hokkaido) to the Kamchatka peninsula are mostly 20–75 km, distances which are probably beyond the dispersal capability of *Epiophlebia*. Sado Island is separated from Honshu (Japan's main island) by 32 km, with a maximum water depth of 200 m. Although the island possessed suitable habitat for *Epiophlebia* within our threshold predictions, the species is absent from the island. Assuming a sea level drop of 140 m within the LGM, the distance between Sado and Honshu was greater than 10 km (Kawauchi, 2024) providing indirect evidence of the dispersal capability of *Epiophlebia*. Furthermore, the remote island of Oki does possess *Epiophlebia*, and was connected to the mainland within the LGM. Finally, Hokkaido and Honshu were hypothesized to be connected by a land bridge during the LGM (Yashima and Miyauchi, 1990). As such, a land bridge within the LGM would still not connect Hokkaido to the Kuril Islands except for Kunashir and Iturup, preventing *Epiophlebia* from dispersing further north.

Increased sampling and population genetics of *Epiophlebia* would illuminate if both refugia were effective habitats throughout the Holocene. Paleo-ecological niche modeling and genetic studies in the context of Asian and Eurasian refugia are rare except in plants and mammals (Anijalg et al., 2018; J. Li et al., 2016; Tang et al., 2018; Wang et al., 2016), the few studies pertaining to insects are in the context of pests (Song et al., 2018).

## Conclusion

ENMs of odonates are still gaining popularity within the scientific literature, which have stressed the importance of their conservation in the context of fire ecology, climate change, and anthropogenic disruption (Abbott et al., 2022; Bush et al., 2014; Cancellario et al., 2022; Collins, 2014; Collins & McIntyre, 2015; Dorji et al., 2020; Goodman et al., 2022; Kalkman et al., 2022; Nidup et al., 2020). Modeling of future odonate distributions has noted habitat loss or extinction within specialized endemic riverine species, and northward range shifting in high dispersal species (Boys & Adam, 2021; Flenner et al., 2010; Hassall & Thompson, 2008; Jaeschke et al., 2013; Kietzka et al., 2018; Simaika & Samways, 2015). A recent ENM study of *E. laidlawi* by Nidup et al. (2020) noted uphill shifting of the species by 500 m by the year 2080, due to temperature increases at the lower elevational range of the species at 2000 m. However, permanent snow cover within the Himalayas occurs at 4000 m, prohibiting further northern expansion of the species to higher elevations. Furthermore, Nidup et al. (2020) estimate 83–90% habitat loss of *E. laidlawi* by 2080, stressing the importance of conservation for not only the habitats of *E. laidlawi*, but utilizing ENMs to highlight areas of high conservation value within data poor countries (Dorji et al., 2020). *Epiophlebia* is a specialized and endemic group, highly susceptible to environmental perturbation due to their narrow habitat ranges, small population sizes, and partivoltinism. Our predictions here are hypotheses that can be evaluated,

refined, and tested. One cannot know whether a given species has responded to climatic changes in the same fashion across its history, which means that our hypotheses are based on current population data and expanding this dataset may result in modifications to our mod-

els. Future studies could utilize our models as a baseline for predictions of future habitat suitability of the genus in the face of habitat destruction.

In our study we present the first present-day distribution model of the relict dragonfly genus *Epiophlebia*.

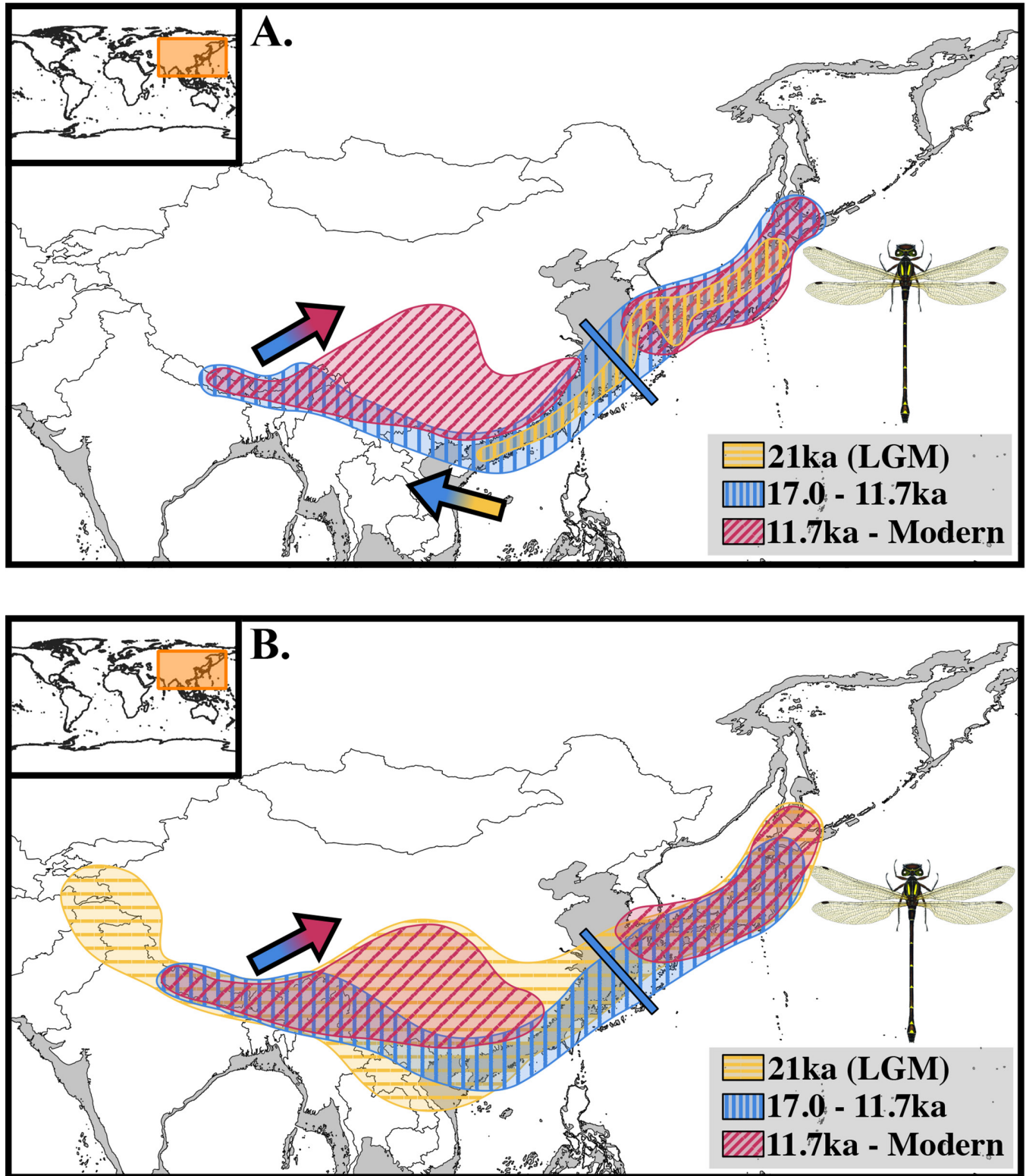


**Figure 6.** Hypothesized distributions of *Epiophlebia* based on our continuous (‘cloglog’) (A) and thresholded (10% omission) (B) predictions since the LGM. Colors represent distributional range within the LGM (hatched yellow), Heinrich Stadial—Younger Dryas (17.0–11.7 ka) (hatched blue), and the Younger Dryas to modern day (11.7–0) (hatched violet). Arrows represent dispersal events to each new range within each time period, while rectangles represent vicariance events. Illustration of *Epiophlebia laidlawi* from Gyetlshen et al. (2017).



Our results indicate several unsampled areas (central China and Sino-Tibetan refuge) which have the potential to harbor new populations of the genus. Furthermore, our results support the hypothesis of Büsse et al. (2012) in which a continuous route of gene flow among disparate populations of *Epiophlebia* was possible during the LGM. Previous research postulated that *Epiophlebia* originated in the Jurassic within Pangaea (Brockhaus & Hartmann, 2009). Although this might be true for fossil ancestors of *Epiophlebia*, molecular data from Büsse et al. (2012) and Büsse & Ware (2022) refute this claim, providing an alternative that extant species originated much more recently. Our data provide an additional layer of support for Büsse et al. (2012) in which genetic admixture of *Epiophlebia* was possible during the last ice age.

### Competing interests

The authors declare no competing interests.

### Acknowledgements

We would like to thank the following for the use of their occurrence and natural history data of *E. superstes* throughout Japan: Arai, K., Arai, Y., Azuma, T., Ehira, K., Fukui, M., Futahashi, R., Higurashi, T., Hisamatsu, S., Horita, M., Ichii, H., Imamura, H., Ishida, K., Ito, S., Kanbe, T., Karube, H., Kita, H., Kojo, T., Kubota, S., Kuranishi, R., Matsuhira, K., Matsuki, K., Mitamura, T., Miyakawa, T., Mochizuki, T., Moriyasu, A., Muraki, A., Murose, A., Nakahara, M., Naraoka, H., Natsume, H., Nishida, T., Ohama, S., Suda, S., Sugimura, M., Tabata, O., Tawada, J., Tsuchiya, K., Tsujitashiro, F., Tsurusaki, N., Usui, T., Watanabe, O., Yagi, T., Yamamoto, E., Yamamoto, T., Yasuda, S., Yanagiya, T., Yoshida, K., Yoshino, T., Yui, M. We would also like to thank Carnaval, A., and Blair, M., for their advice and suggestions for model building and scope of paper. We are also grateful for Kohli, M., for her insight into the biogeography and divergence time of *Epiophlebia*. This work was supported by NSF Awards (Abbott: 2002489; Ware: 2002473; Bybee: 2002432; Guaralnick: 2002457), Genealogy of Odonata (GEODE): Dispersal and color as drivers of 300 million years of global dragonfly evolution.

### Author contributions

Conceptualization: AMG, CDB, SB, HU, JW; Methodology: AMG, MEB; Software: AMG; Validation: AMG, CDB, SB, HU, TM, MEB, JW; Formal analysis: AMG; Investigation: AMG; Resources: JW; Data Curation: AMG; Writing—Original Draft: AMG; Writing—Review and Editing: AMG, CDB, SB, HU, TM, MEB, JW; Visualization: AMG; Supervision: CDB, SB, HU, TM, MEB, JW; Project Administration: JW.

### References

Abbott, J. C., Bota-Sierra, C. A., Guralnick, R., Kalkman, V., González-Soriano, E., Novelo-Gutiérrez, R., . . . Belitz, M. W. (2022). Diversity of Nearctic dragonflies and damselflies (Odonata). *Diversity*, 14(7), 575. doi:10.3390/d14070575

Amano, K. & Mochizuki, T. (2011). Assessing the dependence of fish and benthic animals on water temperature and quality using riverside census results. *River Technology Papers*, 17. [In Japanese].

Anijalg, P., Ho, S. Y., Davison, J., Keis, M., Tammeleht, E., Bobowik, K., . . . Vorobiev, A. A. (2018). Large-scale migrations of brown bears in Eurasia and to North America during the Late Pleistocene. *Journal of Biogeography*, 45(2), 394–405. doi:10.1111/jbi.13126

Asahina, S. (1948). A review of the knowledge of *Epiophlebia sperstes* Selys (II). *Shin-konchu*, 1(5): 35–39. [In Japanese].

Asahina, S. (1954). Morphological study of a relic dragonfly *Epiophlebia superstes* Selys.

Asahina, S. (1961a). Is *Epiophlebia laidlawi* Tillyard (Odonata, Anisozygoptera) a good species? *Internationale Revue der Gesamten Hydrobiologie und Hydrographie*, 46(3), 441–446. doi:10.1002/iroh.19610460310

Asahina, S. (1961b). The taxonomic characteristics of the Himalayan *Epiophlebia*-larva (Insecta, Odonata). *Proceedings of the Japan Academy*, 37(1), 42–42. [In Japanese]. doi:10.2183/pjab1945.37.42

Bechly, G. (1996a). Fossil odonates in Tertiary amber. *Petalura*, 2, 1–15.

Bechly, G. (1996b). Morphologische Untersuchungen am Flügelgeäder der rezenten Libellen und deren Stammgruppenvertreter (Insecta; Pterygota; Odonata) unter besonderer Berücksichtigung der phylogenetischen Systematik und des Grundplanes der Odonata. *Petalura*, 1–402.

Bintanja, R., Van De Wal, R. S. & Oerlemans, J. (2005). Modelled atmospheric temperatures and global sea levels over the past million years. *Nature*, 437(7055), 125–128. doi:10.1038/nature03975

Blanke, A., Beckmann, F. & Misof, B. (2013). The head anatomy of *Epiophlebia superstes* (Odonata: Epiophlebiidae). *Organisms Diversity & Evolution*, 13, 55–66. doi:10.1007/s13127-012-0097-z

Blanke, A., Büsse, S. & Machida, R. (2015). Coding characters from different life stages for phylogenetic reconstruction: a case study on dragonfly adults and larvae, including a description of the larval head anatomy of *Epiophlebia superstes* (Odonata: Epiophlebiidae). *Zoological Journal of the Linnean Society*, 174(4), 718–732. doi:10.1111/zoj.12258

Blanke, A., Greve, C., Mokso, R., Beckmann, F. & Misof, B. (2013). An updated phylogeny of Anisoptera including formal convergence analysis of morphological characters. *Systematic Entomology*, 38(3), 474–490. doi:10.1111/syen.12012

Booth, T. H. (2022). Checking bioclimatic variables that combine temperature and precipitation data before their use in species distribution models. *Austral Ecology*, 47(7), 1506–1514. doi:10.1111/aec.13234

Boys, W. A. & Adam, M. (2021). Predicting the distributions of regional endemic dragonflies using a combined model approach. *Insect Conservation and Diversity*, 14(1), 52–66. https://doi.org/10.1111/icad.12444

Brame, H.-M. R. & Stigall, A. L. (2014). Controls on niche stability in geologic time: congruent responses to biotic and abiotic environmental changes among Cincinnatian (Late Ordovician) marine invertebrates. *Paleobiology*, 40(1), 70–90. doi:10.1666/13035

Brockhaus, T. & Hartmann, A. (2009). New records of *Epiophlebia laidlawi* Tillyard in Bhutan, with notes on its biology, ecology, distribution, zoogeography and threat status (Anisozygoptera: Epiophlebiidae). *Odonatologica*, 38(3), 203–215.

Brown, J. L., Hill, D. J., Dolan, A. M., Carnaval, A. C. & Haywood, A. M. (2018). PaleoClim, high spatial resolution paleoclimate surfaces for global land areas. *Scientific Data*, 5(1), 1–9. doi:10.1038/sdata.2018.254

Büsse, S. (2016). Morphological re-examination of *Epiophlebia laidlawi* (Insecta: Odonata) including remarks on taxonomy. *International Journal of Odonatology*, 19(4), 221–238. doi:10.1080/13887890.2016.1257442

- Büsse, S., Helmker, B. & Hörnschemeyer, T. (2015). The thorax morphology of *Epiophlebia* (Insecta: Odonata) nymphs—including remarks on ontogenesis and evolution. *Scientific Reports*, 5(1), 1–14. doi:10.1038/srep12835
- Büsse, S., von Grumbkow, P., Hummel, S., Shah, D. N., Tachamo Shah, R. D., Li, J., . . . Hörnschemeyer, T. (2012). Phylogeographic analysis elucidates the influence of the Ice Ages on the disjunct distribution of relict dragonflies in Asia. *PLoS One*, 7(5), e38132. doi:10.1371/journal.pone.0038132
- Büsse, S. & Ware, J. L. (2022). Taxonomic note on the species status of *Epiophlebia diana* (Insecta, Odonata, Epiophlebiidae), including remarks on biogeography and possible species distribution. *ZooKeys*, 1127, 79–90. doi:10.3897/zookeys.1127.83240
- Bush, A. A., Nipperess, D. A., Duursma, D. E., Theischinger, G., Turak, E. & Hughes, L. (2014). Continental-Scale Assessment of Risk to the Australian Odonata from Climate Change. *PLoS One*, 9(2), e88958. doi:10.1371/journal.pone.0088958
- Bybee, S., Córdoba-Aguilar, A., Duryea, M. C., Futahashi, R., Hansson, B., Lorenzo-Carballa, M. O., . . . Svensson, E. I. (2016). Odonata (dragonflies and damselflies) as a bridge between ecology and evolutionary genomics. *Frontiers in zoology*, 13(1), 1–20. doi:10.1186/s12983-016-0176-7
- Bybee, S. M., Kalkman, V. J., Erickson, R. J., Frandsen, P. B., Breinholt, J. W., Suvorov, A., . . . Abbott, J. C. (2021). Phylogeny and classification of Odonata using targeted genomics. *Molecular Phylogenetics and Evolution*, 160, 107115. doi:10.1016/j.ympev.2021.107115
- Bybee, S. M., Ogden, T. H., Branham, M. A. & Whiting, M. F. (2008). Molecules, morphology and fossils: a comprehensive approach to odonate phylogeny and the evolution of the odonate wing. *Cladistics*, 24(4), 477–514. doi:10.1111/j.1096-0031.2007.00191.x
- Cancellario, T., Miranda, R., Baquero, E., Fontaneto, D., Martínez, A. & Mammola, S. (2022). Climate change will redefine taxonomic, functional, and phylogenetic diversity of Odonata in space and time. *npj Biodiversity*, 1(1), 1. doi:10.1038/s44185-022-00001-3
- Carle, F. L. (2012). A new *Epiophlebia* (Odonata: Epiophlebioidea) from China with a review of epiophlebian taxonomy, life history, and biogeography. *Arthropod Systematics & Phylogeny*, 70(2), 75–83. doi:10.3897/asp.70.e31750
- Chen, L., Wu, S. & Pan, T. (2011). Variability of climate–growth relationships along an elevation gradient in the Changbai Mountain, northeastern China. *Trees*, 25, 1133–1139. doi:10.1007/s00468-011-0588-0
- Clark, P. U., Dyke, A. S., Shakun, J. D., Carlson, A. E., Clark, J., Wohlfarth, B., . . . McCabe, A. M. (2009). The last glacial maximum. *Science*, 325(5941), 710–714. doi:10.1126/science.1172873
- Collen, B., Whitton, F., Dyer, E. E., Baillie, J. E. M., Cumberlidge, N., Darwall, W. R. T., . . . Böhm, M. (2014). Global patterns of freshwater species diversity, threat and endemism. *Global Ecology and Biogeography*, 23(1), 40–51. doi:10.1111/geb.12096
- Collins, S. D. (2014). *Fine-scale modeling of riverine Odonata distributions in the northeastern United States*. (Thesis). Texas Tech University
- Collins, S. D. & McIntyre, N. E. (2015). Modeling the distribution of odonates: a review. *Freshwater Science*, 34(3), 1144–1158. doi:10.1086/682688
- Córdoba-Aguilar, A., Beatty, C. & Bried, J. (2023). *Dragonflies and damselflies: model organisms for ecological and evolutionary research*. Oxford University Press. doi:10.1093/oso/9780192898623.001.0001
- Davies, A. (1992). *Epiophlebia laidlawi*—Flying. *Kimminsia*, 3(2), 10–11.
- Dijkstra, K.-D. B., Bechly, G., Bybee, S. M., Dow, R. A., Dumont, H. J., Fleck, G., . . . Ware, J. (2013). The classification and diversity of dragonflies and damselflies (Odonata). *Zootaxa*, 3703(36), 45. doi:10.11646/zootaxa.3703.1.9
- Dorji, T. (2015). New distribution records of *Epiophlebia laidlawi* Tillyard, 1921 (Insecta: Odonata) in Bhutan. *Journal of Threatened Taxa*, 7(10), 7668–7675. doi:10.11609/JoTT.o4092.7668-75
- Dorji, T., Linke, S. & Sheldon, F. (2020). Optimal model selection for Maxent: a case of freshwater species distribution modelling in Bhutan, a data poor country. *Authorea Preprints*. doi:10.22541/au.160551779.93380163/v1
- Dudei, N. L. & Stigall, A. L. (2010). Using ecological niche modeling to assess biogeographic and niche response of brachiopod species to the Richmondian Invasion (Late Ordovician) in the Cincinnati Arch. *Palaeogeography, Palaeoclimatology, Palaeoecology*, 296(1–2), 28–43. doi:10.1016/j.palaeo.2010.06.012
- Dudley, R. & Yanoviak, S. P. (2011). Animal aloft: the origins of aerial behavior and flight. *Integrative and Comparative Biology*, 51(6), 926–936. doi:10.1093/icb/002
- Elith, J., Kearney, M. & Phillips, S. (2010). The art of modelling range-shifting species. *Methods in Ecology and Evolution*, 1(4), 330–342. doi:10.1111/j.2041-210X.2010.00036.x
- Fick, S. E. & Hijmans, R. J. (2017). WorldClim 2: new 1-km spatial resolution climate surfaces for global land areas. *International journal of climatology*, 37(12), 4302–4315. doi:10.1002/joc.5086
- Fleck, G., Li, J., Schorr, M., Nel, A., Zhang, X., Lin, L. & Gao, M. (2013). *Epiophlebia sinensis* Li & Nel 2011. In Li, et al. (Eds) (2012), (*Odonata*) newly recorded in North Korea. pp. 1–4. *International Dragonfly Fund Report*, 61.
- Flenner, I., Richter, O. & Suhling, F. (2010). Rising temperature and development in dragonfly populations at different latitudes. *Freshwater Biology*, 55(2), 397–410. doi:10.1111/j.1365-2427.2009.02289.x
- Futahashi, R. (2004). The dragonflies and damselflies of Toyama Prefecture, central Honshu, Japan. *Special publications from the Toyama Science Museum*, 17, 1–220. [In Japanese].
- Futahashi, R., Kawahara-Miki, R., Kinoshita, M., Yoshitake, K., Yajima, S., Arikawa, K. & Fukatsu, T. (2015). Extraordinary diversity of visual opsin genes in dragonflies. *Proceedings of the National Academy of Sciences*, 112(11), E1247–E1256. doi:10.1073/pnas.1424670112
- Goodman, A. M., Kass, J. M. & Ware, J. (2022). Dynamic distribution modelling of the swamp tigertail dragonfly *Synthemis eustalacta* (Odonata: Anisoptera: Synthemistidae) over a 20-year bushfire regime. *Ecological Entomology*, 48(2), 209–225. doi:10.1111/een.13216
- Gose, K. (1953). *Epiophlebia superstes* in Nara Prefecture. *Kansai Sizennkagaku*, 7, 35. [In Japanese].
- Grimaldi, D., Engel, M. S. (2005). *Evolution of the Insects*. Cambridge University Press.
- Guisan, A. & Thuiller, W. (2005). Predicting species distribution: offering more than simple habitat models. *Ecology Letters*, 8(9), 993–1009. doi:10.1111/j.1461-0248.2005.00792.x
- Guisan, A. & Zimmerman, N. E. (2000). Predictive habitat distribution models in ecology. *Ecological Modelling*, 135, 147–186. doi:10.1016/S0304-3800(00)00354-9
- Gyeltshen, T., Kalkman, V. & Orr, A. (2017). *A field guide to the common dragonflies & damselflies of Bhutan*. National Biodiversity Centre (NBC).
- Hamada, K. & Inoue, K. (1985). *The dragonflies of Japan in colour*. Vols. I and II. Kodansha, Tokyo. [In Japanese].

- Hassall, C. & Thompson, D. J. (2008). The effects of environmental warming on Odonata: a review. *International Journal of Odonatology*, 11(2), 131–153. doi:10.1080/13887890.2008.9748319
- Ikeda, H. (1998). Himalayan Potentilla and its relation to the sino-Japanese floristic region. University Museum. *The University of Tokyo Bulletin*, 37, 139–146.
- Ishida S., Ichihashi, H., Ohkawa, C., Nakane, T., Naruse, Z., Matoba, T. (1959). Kihoku-Kinan survey committee collected records. *Hirakura*, 3(25), 4–16. [In Japanese].
- Jaeschke, A., Bittner, T., Reineking, B. & Beierkuhnlein, C. (2013). Can they keep up with climate change? Integrating specific dispersal abilities of protected Odonata in species distribution modelling. *Insect Conservation and Diversity*, 6(1), 93–103. doi:10.1111/j.1752-4598.2012.00194.x
- Kalkman, V. J., Boudot, J.-P., Futahashi, R., Abbott, J. C., Bota-Sierra, C. A., Guralnick, R., . . . Belitz, M. W. (2022). Diversity of Palaearctic dragonflies and damselflies (Odonata). *Diversity*, 14(11), 966. doi:10.3390/d14110966
- Karger, D. N., Conrad, O., Böhrner, J., Kawohl, T., Kreft, H., Soria-Auza, R. W., . . . Kessler, M. (2017). Climatologies at high resolution for the earth's land surface areas. *Scientific Data*, 4(1), 1–20. doi:10.1038/sdata.2017.122
- Karger, D. N., Nobis, M. P., Normand, S., Graham, C. H. & Zimmermann, N. E. (2023). CHELSA-TraCE21k—high-resolution (1 km) downscaled transient temperature and precipitation data since the Last Glacial Maximum. *Climate of the Past*, 19(2), 439–456. doi:10.5194/cp-19-439-2023
- Kass, J. M., Muscarella, R., Galante, P. J., Bohl, C. L., Pinilla-Buitrago, G. E., Boria, R. A., . . . Anderson, R. P. (2021). ENMeval 2.0: Redesigned for customizable and reproducible modeling of species' niches and distributions. *Methods in Ecology and Evolution*, 12(9), 1602–1608. doi:10.1111/2041-210X.13628
- Kawauchi, K. (2024). Seismo-Tectonics on the Eastern Japan Sea Plate Boundary. My view about Seismicity around Niiigata Region. Lost Land, The Meaning of the Islands in the Kohei Map. (In Japanese). <https://kanbara.sakura.ne.jp/page1.html>
- Kietzka, G. J., Pryke, J. S. & Samways, M. J. (2018). Comparative effects of urban and agricultural land transformation on Odonata assemblages in a biodiversity hotspot. *Basic and Applied Ecology*, 33, 89–98. doi:10.1016/j.baae.2018.08.008
- Kohli, M., Djernæs, M., Herrera, M. S., Sahlen, G., Pilgrim, E., Simonsen, T. J., . . . Ware, J. (2021). Comparative phylogeography uncovers evolutionary past of Holarctic dragonflies. *PeerJ*, 9, e11338. doi:10.7717/peerj.11338
- Lattin, G. d. (1967). *Grundriss der Zoogeographie*. Jena: Gustav Fischer Verlag.
- Letsch, H., Gottsberger, B. & Ware, J. L. (2016). Not going with the flow: a comprehensive time-calibrated phylogeny of dragonflies (Anisoptera: Odonata: Insecta) provides evidence for the role of lentic habitats on diversification. *Molecular Ecology*, 25(6), 1340–1353. doi:10.1111/mec.13562
- Li, J., McCarthy, T. M., Wang, H., Weckworth, B. V., Schaller, G. B., Mishra, C., . . . Beissinger, S. R. (2016). Climate refugia of snow leopards in High Asia. *Biological Conservation*, 203, 188–196. doi:10.1016/j.biocon.2016.09.026
- Li, J. K., Nel, A., Zhang, X. P., Fleck, G., GAO, M. X., Lin, L. & Zhou, J. (2012). A third species of the relict family Epiophlebiidae discovered in China (Odonata: Epiproctophora). *Systematic Entomology*, 37(2), 408–412. doi:10.1111/j.1365-3113.2011.00610.x
- Lobo, J. M., Jiménez-Valverde, A. & Real, R. (2008). AUC: a misleading measure of the performance of predictive distribution models. *Global Ecology and Biogeography*, 17(2), 145–151. doi:10.1111/j.1466-8238.2007.00358.x
- Lohmann, H. (1996). Das phylogenetische system der Anisoptera (Odonata). *Entomologische Zeitschrift*, 106, 209–266.
- Mahato, M. (1993). *Epiophlebia laidlawi*—a living ghost. *Selysia*, 22(1), 2–2.
- Matsuhira, M. (1996). Distribution survey of rare dragonflies on the Osumi Peninsula. *Charitable Trust TaKaRa Harmonist Fund 1995 Research Activity Report*, 37–46. [In Japanese].
- Myers, C. E., Stigall, A. L. & Lieberman, B. S. (2015). PaleoENM: applying ecological niche modeling to the fossil record. *Paleobiology*, 41(2), 226–244. doi:10.1017/pab.2014.19
- Naimi, B. (2017). *Package 'usdm': Uncertainty Analysis for Species Distribution Models*. Wien: [cran.r-project.org](http://cran.r-project.org).
- Needham, J. G. (1930). Manual of the dragonflies of China. A monographic study of the Chinese Odonata. *Acta Zoologica Sinica A*, 11, 1–399.
- Nel, A. (1993). Les “Anisozygoptera” fossiles: phylogénie et classification (Odonata). *Martinia*, 3, 1–311.
- Nicholson, D. B., Ross, A. J. & Mayhew, P. J. (2014). Fossil evidence for key innovations in the evolution of insect diversity. *Proceedings of the Royal Society B: Biological Sciences*, 281(1793), 20141823. doi:10.1098/rspb.2014.1823
- Nidup, T., Tamang, D. T., Tobgay, S., Ba-jgai, R. C., Wangmo, S., Dorji, T. & Wangchuk, K. (2020). Abundance and distribution of threatened *Epiophlebia laidlawi* Tillyard, 1921 (Odonata: Epiophlebiidae) in Eastern Bhutan. *Sherub Doenme: The Research Journal of Sherubtse College*, 13(1).
- O'Donnell, M. S. & Ignizio, D. A. (2012). Bioclimatic predictors for supporting ecological applications in the conterminous United States. *US geological survey data series*, 691(10), 4–9. doi:10.3133/ds691
- Okazawa, T. (1974). Studies on the Aquatic Insects in the Stream Hoshioki near Sapporo (With 3 Text-figures and 3 Tables). *Journal of the Faculty of Science Hokkaido University Series VI. Zoology* 19(2), 474–488.
- Ozono, A., Kawashima, I. & Futahashi, R. (2021). *Dragonflies of Japan*. Revised edition. Tokyo: Bunichi-Sogo Syuppan., Co. Ltd. [In Japanese].
- Peterson, A. T. & Soberón, J. (2012). Species Distribution Modeling and Ecological Niche Modeling: Getting the Concepts Right. *Natureza & Conservação*, 10(2), 102–107. doi:10.4322/natcon.2012.019
- Phillips, S. J. (2021). A brief tutorial on Maxent. *AT&T Research*, 190(4), 231–259.
- Phillips, S. J., Anderson, R. P., Dudík, M., Schapire, R. E. & Blair, M. E. (2017). Opening the black box: an open-source release of Maxent. *Ecography*, 40(7), 887–893. doi:10.1111/ecog.03049
- Purcell, C. K. & Stigall, A. L. (2021). Ecological niche evolution, speciation, and feedback loops: Investigating factors promoting niche evolution in Ordovician brachiopods of eastern Laurentia. *Palaeogeography, Palaeoclimatology, Palaeoecology*, 578, 110555. doi:10.1016/j.palaeo.2021.110555
- Radosavljevic, A. & Anderson, R. P. (2014). Making better Maxent models of species distributions: complexity, overfitting and evaluation. *Journal of Biogeography*, 41(4), 629–643. doi:10.1111/jbi.12227
- R Core Team (2021). *R: A language and environment for statistical computing*. R Foundation for Statistical Computing, Vienna, Austria. 2012. [cran.r-project.org/](http://cran.r-project.org/)
- Rehn, A. C. (2003). Phylogenetic analysis of higher-level relationships of Odonata. *Systematic Entomology*, 28(2), 181–240. doi:10.1046/j.1365-3113.2003.00210.x
- Schmidt, M. & Hertzberg, J. (2011). Abrupt climate change during the last ice age. *Nature education knowledge*, 3(11).



- Selys Longchamps, E. de (1889). Palaeophlebia. Nouvelle légion de Caloptérygines. Suivi de la description d'une nouvelle gomphine du Japon: Tachopteryx Pryeri. *Annales de la Société entomologique de Belgique*, 33, 153.
- Shah, R. D. T., Narayan Shah, D. & Domisch, S. (2012). Range shifts of a relict Himalayan dragonfly in the Hindu Kush Himalayan region under climate change scenarios. *International Journal of Odonatology*, 15(3), 209–222. doi:10.1080/13887890.2012.697399
- Simaika, J. P. & Samways, M. J. (2015). Predicted range shifts of dragonflies over a wide elevation gradient in the southern hemisphere. *Freshwater Science*, 34(3), 1133–1143. doi:10.1086/682686
- Song, W., Cao, L.-J., Li, B.-Y., Gong, Y.-J., Hoffmann, A. A. & Wei, S.-J. (2018). Multiple refugia from penultimate glaciations in East Asia demonstrated by phylogeography and ecological modelling of an insect pest. *BMC Evolutionary Biology*, 18(1), 1–16. doi:10.1186/s12862-018-1269-z
- Stigall, A. L. (2012). Using ecological niche modelling to evaluate niche stability in deep time. *Journal of Biogeography*, 39(4), 772–781. doi:10.1111/j.1365-2699.2011.02651.x
- Tang, C. Q., Matsui, T., Ohashi, H., Dong, Y.-F., Momohara, A., Herando-Moraira, S., . . . Luu, H. T. (2018). Identifying long-term stable refugia for relict plant species in East Asia. *Nature Communications*, 9(1), 1–14. doi:10.1038/s41467-018-06837-3
- Tani, K. & Miyatake, Y. (1979). The discovery of *Epiophlebia laidlawi* Tillyard, 1921 in the Kathmandu Valley, Nepal (Anisozygoptera: Epiophlebiidae). *Odonatologica*, 8(4), 329–332.
- Tillyard, R. (1921). On an anisozygopterous larva from the Himalayas (Order Odonata). *Records of the Zoological Survey of India*, 22(2), 93–107. doi:10.26515/rzsi/v22/i2/1921/163517
- Tokuyama, Y. (1992). Aquatic Insects in the Handa River System—Comprehensive Academic Survey Report. *Handamachi Kyoudo-kennkyuu Happyoukai Kiyou*, 43, 111–121. [In Japanese].
- Tomita, S., Yamashita, A., Ishibashi, K., Miki, T., Takahashi, R., Shuto, T., . . . Igarashi, C. (1975). Submarine geology west of the Tsushima Islands. *Science reports, Department of Geology, Kyushu University*, 12, 77–90.
- Ubukata, H. & Miyazaki, T. (in press). Review: Thresholds in latitude, altitude, water and air temperature of the distribution records of *Epiophlebia superstes* (Selys, 1889) in the Japanese Archipelago. *Tombo Acta Odonatologica Japonica*. 67. [In Japanese with English summary].
- Valavi, R., Guillera-Arroita, G., Lahoz-Monfort, J. J. & Elith, J. (2021). Predictive performance of presence-only species distribution models: a benchmark study with reproducible code. *Ecological Monographs*, 92(0), e01486. doi:10.1002/ecm.1486
- Wang, W.-T., Xu, B., Zhang, D.-Y. & Bai, W.-N. (2016). Phylogeography of postglacial range expansion in *Juglans mandshurica* (Juglandaceae) reveals no evidence of bottleneck, loss of genetic diversity, or isolation by distance in the leading-edge populations. *Molecular Phylogenetics and Evolution*, 102, 255–264. doi:10.1016/j.ympev.2016.06.005
- Warren, D. L., Glor, R. E. & Turelli, M. (2010). ENMTools: a toolbox for comparative studies of environmental niche models. *Ecography*, 33(3), 607–611. doi:10.1111/j.1600-0587.2009.06142.x
- Warren, D. L. & Seifert, S. N. (2011). Ecological niche modeling in Maxent: the importance of model complexity and the performance of model selection criteria. *Ecological Applications*, 21(2), 335–342. doi:10.1890/10-1171.1
- Yamaura, T., Kimura, N., Sasaki, H. & Kitamura, J. (2009). Habitation monitoring survey report for aquatic organisms in Shiroyama National Forest Kurokigazawa. *Chūbu region forest management office*. [In Japanese]. [rinya.maff.go.jp/chubu/kiso\\_fc/kiso\\_fc/attach/pdf/tyousahoukoku-1.pdf](http://rinya.maff.go.jp/chubu/kiso_fc/kiso_fc/attach/pdf/tyousahoukoku-1.pdf)
- Yashima, K. & Miyauchi, T. (1990). The Tsugaru land bridge problem related to Quaternary coastal tectonics, northeast Japan. *The Quaternary Research (Daiyonki-Kenkyu)*, 29(3), 267–275. [In Japanese with English summary]. <https://doi.org/10.4116/jaqua.29.267>
- Zurell, D., Franklin, J., König, C., Bouchet, P. J., Dormann, C. F., Elith, J., . . . Guisan, A. (2020). A standard protocol for reporting species distribution models. *Ecography*, 43(9), 1261–1277. doi:10.1111/ecog.04960

### Supplementary Material

Supplemental Figure S1. Permutation analysis and response curves of the most important variables from our optimal maxent model of *Epiophlebia*. Maxent calculates permutation importance by changing the values of each environmental variable at random, then calculating the difference using the AUC from the 'training data'. The values of each environmental variable are randomly permuted within the training presence and background data, the resultant drop in training AUC is calculated, then normalized to percentages (Phillips et al., 2017). Bar graphs represent normalized percentages of variables possessing non-zero lambda values. Response curves show how each environmental variable individually affects the maxent prediction in terms of increasing or decreasing suitability. Behavior of response curve is dictated by model complexity (feature classes and regularization multipliers). Variables follow Worldclim v2 (Fick & Hijmans, 2017). Bioclimatic variable bio04 (Temperature Seasonality) has been multiplied by 100 to keep significant figures (O'Donnell & Ignizio, 2012).

Supplemental Figure S2. Permutation analysis and response curves of the most important variables from our optimal maxent model of *Epiophlebia laidlawi*. Maxent calculates permutation importance by changing the values of each environmental variable at random, then calculating the difference using the AUC from the 'training data'. The values of each environmental variable are randomly permuted within the training presence and background data, the resultant drop in training AUC is calculated, then normalized to percentages (Phillips et al., 2017). Bar graphs represent normalized percentages of variables possessing non-zero lambda values. Response curves show how each environmental variable individually affects the maxent prediction in terms of increasing or decreasing suitability. Behavior of response curve is dictated by model complexity (feature classes and regularization multipliers). Variables follow Worldclim v2 (Fick & Hijmans, 2017). Bioclimatic variable bio04 (Temperature Seasonality) has been multiplied by 100 to keep significant figures (O'Donnell & Ignizio, 2012).

Supplemental Figure S3. Permutation analysis and response curves of the most important variables from our optimal maxent model of *Epiophlebia superstes*. Maxent calculates permutation importance by changing the values of each environmental variable at random, then calculating the difference using the AUC from the 'training data'. The values of each environmental variable are randomly permuted within the training presence and background data, the resultant drop in training AUC is calculated, then normalized to percentages (Phillips et al., 2017). Bar graphs represent normalized percentages of variables possessing non-zero lambda values. Response curves show how each environmental variable individually affects the maxent prediction in terms of increasing or decreasing suitability. Behavior of response curve is dictated by model complexity (feature classes and regularization multipliers). Variables follow Worldclim v2 (Fick & Hijmans, 2017). Bioclimatic variable bio04 (Temperature Seasonality) has been multiplied by 100 to keep significant figures (O'Donnell & Ignizio, 2012).